CONFIDENTIAL

Copy 372
RM L56F11

NACA RM L56F11

NACA

CASE FILE
COPY

RESEARCH MEMORANDUM

HINGE MOMENT AND EFFECTIVENESS OF AN UNSWEPT CONSTANT-CHORD CONTROL AND AN OVERHANG-BALANCED, SWEPT HINGE-LINE CONTROL ON AN 80° SWEPT POINTED WING AT MACH NUMBERS FROM 0.75 TO 1.96

By Lawrence D. Guy

Langley Aeronautical Laboratory
Langley Field, Va.

CLASSIFICATION CHANGED TO UNCLASSIFIED
AUTHORITY: NACA RESEARCH ABSTRACT NO. 128
EFFECTIVE DATE: JUNE 24, 1958
TIM WHL

CLASSIFIED DOCUMENT

This material contains information affecting the National Defense of the United States within the meaning of the espionage laws, Title 18, U.S.C., Secs. 793 and 794, the transmission or revelation of which in any manner to an unauthorized person is prohibited by law.

NATIONAL ADVISORY COMMITTEE
FOR AERONAUTICS

WASHINGTON

August 28, 1956

CONFIDENTIAL

NATIONAL ADVISORY COMMITTEE FOR AERONAUTICS

RESEARCH MEMORANDUM

HINGE MOMENT AND EFFECTIVENESS OF AN UNSWEPT CONSTANT-CHORD CONTROL AND AN OVERHANG-BALANCED, SWEPT HINGE-LINE CONTROL ON AN 80° SWEPT POINTED WING AT MACH NUMBERS FROM 0.75 TO 1.96

By Lawrence D. Guy

SUMMARY

An investigation of a semispan-wing—fuselage model having an 80° swept pointed wing with either an unbalanced constant-chord control or an overhang-balanced swept hinge-line control was conducted in the Langley 9- by 12-inch blowdown tunnel. Control hinge moments and effectiveness characteristics were obtained over an angle-of-attack range of ±16° at control deflections up to 25°. Data were obtained at Mach numbers from 0.75 to 1.96.

Both controls were effective throughout the Mach number range to the highest angles of attack and control deflections tested. The use of sweepback and taper in the overhang-balanced control resulted in hinge moment and effectiveness characteristics which appeared more desirable than those exhibited in previous tests of unswept, untapered overhang-balanced controls. The tapered overhang which balanced the control hinge moments at subsonic speeds introduced no severe nonlinearities in the variations with control deflection of hinge moment, of rolling moment, or of lift. The sweepback of the hinge line effectively reduced, at transonic speeds, the increase in hinge moment with Mach number associated with the rearward and outward shift of the center of pressure. Comparison of the hinge moments, for both of the controls acting as ailerons, deflected to produce a given rate of roll, showed much smaller hinge moments and less change in hinge moments with Mach number for the balanced control at transonic and low supersonic speeds. At the highest Mach number, however, the advantages to the balanced control were decreased. Comparison on the basis of deflection work for the same roll rate showed little advantage to the balanced control at supersonic speeds because of the large required deflection.

INTRODUCTION

At the very high flight speeds of present-day aircraft and missiles the forces and moments required to actuate control surfaces have become increasingly larger. Attempts to reduce the hinge moments of trailing-edge controls at supersonic speeds by aerodynamic means have generally resulted in controls that have overbalanced and frequently nonlinear hinge-moment characteristics at subsonic speeds (for example see refs. 1, 2, and 3). A need therefore exists for developing control configurations having only a small change in hinge-moment balancing effectiveness at transonic speeds together with good lift and rolling effectiveness at supersonic speeds. The use of a highly swept hinge line appears promising in minimizing the hinge moments which result from the rearward and outward movement of the center of pressure at transonic speeds (ref. 4). Sweeping the control leading edge a greater amount than the hinge line would provide aerodynamic balance and tend to minimize nonlinearity in the hinge-moment variations, usually associated with the sudden unporting of overhang balances, by providing progressive unporting of the control nose as the control is deflected. An 80° swept pointed wing with a control incorporating these features has, therefore, been investigated at transonic and supersonic speeds in the Langley 9- by 12-inch blowdown tunnel. The control had 40° sweepback of the hinge line and a tapered-nose overhang-balanced surface ahead of the hinge line. A second unswept, unbalanced control was also tested and used for comparison.

Hinge-moment and effectiveness characteristics of both controls were obtained over an angle-of-attack range of $\pm 16^\circ$ for control deflections up to 25°. The tests were made at Mach numbers from 0.75 to 1.96 for a range of Reynolds numbers between 3.2×10^6 and 4.4×10^6.

COEFFICIENTS AND SYMBOLS

C_L lift coefficient, $\frac{\text{Lift}}{qS}$

C_D drag coefficient, $\frac{\text{Drag}}{qS}$

C_m pitching-moment coefficient (pitching-moment reference axis located at $0.25\bar{c}$ of the delta wing), $\frac{\text{Pitching moment}}{qS\bar{c}}$

$C_{l_{gross}}$ gross rolling-moment coefficient (rolling-moment reference axis shown in fig. 1), $\frac{\text{Semispan-model rolling moment}}{2qSb}$

C_h control hinge-moment coefficient, $\frac{\text{Hinge moment}}{2M_a q}$

$C_l, \Delta C_L, \Delta C_m$ increment in gross rolling-moment coefficient, lift coefficient, and pitching-moment coefficient, respectively, due to deflection of control surface

ΔC_D increment in drag coefficient due to angle of attack and/or deflection

q free-stream dynamic pressure

S semispan-wing area (including area blanketed by half-body of revolution)

S_a area of control

c local wing chord

$\bar{c}$ mean aerodynamic chord of wing

b wing span, twice distance from rolling-moment reference axis to wing tip

M Mach number

ΔM maximum deviation from average test-section Mach number

M_a moment of area of control back of hinge axis about hinge axis

A wing aspect ratio

M_{a_1} moment of area of control about the control leading edge

M_{a_2} value of M_a for unbalanced control

p roll velocity, radians/sec

α angle of attack, deg

δ control-surface deflection measured perpendicular to hinge line from wing-chord plane (positive trailing edge down), deg

R Reynolds number based on mean aerodynamic chord of wing

W deflection work, $2M_{aq}\left[\int_0^{\delta} C_h \, d\left(\frac{\delta}{57.3}\right) + \int_0^{-\delta} C_h \, d\left(\frac{\delta}{57.3}\right)\right]$

Subscripts:

α partial derivative of coefficient with respect to α

δ partial derivative of coefficient with respect to δ

DESCRIPTION OF MODELS

The principal dimensions of the semispan-wing—body combinations are given in figure 1 and a photograph of one of the models is shown in figure 2. The basic wing (fig. 1) had a delta plan form with 80° leading-edge sweepback and a corresponding aspect ratio of 0.70. The symmetrical airfoil had modified round-nosed hexagonal sections 3 percent thick at the root and 4.88 percent thick at 0.95 b/2. A second model used the basic wing plan form and airfoil sections, the plan form being modified by removal of 5.9 percent of the wing chord at the trailing edge which left the trailing edge blunt. The aspect ratio was approximately 0.77. (See fig. 1.) The wing, exclusive of the control surface, was made of solid steel for both models. A fuselage consisting of a half-body of revolution together with a 0.25-inch shim was integral with the wing for all tests.

The basic delta-wing model had a constant-chord control surface located at the wing trailing edge and extending outboard from fuselage to wing tip. The modified wing model was equipped with a triangular, overhang-balanced control having 40° hinge-line sweepback. Both controls were machined from heat-treated steel and hinged to the wing by a 0.016-inch-diameter steel pin at or near the outboard ends. At the inboard end, a 0.109-inch-diameter shaft, integral with the control surface, was supported by a bearing within the test body and restrained by a clamp.

TEST TECHNIQUE

The semispan model was cantilevered from a five-component strain-gage balance set flush with the tunnel floor. The aerodynamic forces and moments on the semispan-wing—body combinations were measured with respect to the body axes and then rotated to the wind axes. The 0.25-inch shim was used to minimize the effects of the tunnel-wall boundary layer on the flow over the fuselage (refs. 5 and 6). A clearance gap of 0.010 to 0.020 inch was maintained between the fuselage shim and the tunnel floor.

Control-surface hinge moments were measured by means of an electrical strain-gage beam which formed part of the clamp restraining the control-surface shaft and which was contained within the test body. For all tests the Mach number and control deflection were preset and the angle of attack was varied.

TUNNEL AND TEST CONDITIONS

The tests were conducted in the Langley 9- by 12-inch blowdown tunnel which operated from the compressed air of the Langley 19-foot pressure tunnel. The absolute stagnation pressure of the air entering the test section ranged from 2 to $2\frac{1}{3}$ atmospheres. The compressed air was conditioned to insure condensation-free flow in the test section by being passed through a silica-gel drier and then through banks of finned electrical heaters. Criteria for condensation-free flow were obtained from reference 7. Turbulence damping screens were located in the settling chamber. Four interchangeable nozzle blocks provided test-section Mach numbers of 0.70 to 1.25, 1.41, 1.62, and 1.96.

Transonic Nozzle

A description of the transonic nozzle, which has a 7- by 10-inch test section, together with a discussion of the flow characteristics obtained from limited calibration tests, is presented in reference 1. Satisfactory test-section flow characteristics are indicated from the minimum Mach number ($M \approx 0.7$) to about $M = 1.25$. The maximum deviations from the average Mach number in the region occupied by the model are shown in figure 3(a). Limited tests indicate that the stream angle probably did not exceed $\pm 0.1^\circ$ at any Mach number. As the model angle of attack was changed from 0 to $\pm 16^\circ$, the test-section Mach number decreased by an amount not exceeding 0.01. The variation with Mach number of the average Reynolds number of the tests is given in figure 3(b) within $\pm 0.3 \times 10^6$.

Supersonic Nozzles

Test-section flow characteristics of the three supersonic fixed Mach number nozzles which had 9- by 12-inch test sections were determined from extensive calibration tests and are reported in reference 8. Deviation of flow conditions in the test section with the tunnel clear and model test Reynolds numbers are presented in the following table:

Average Mach number	1.41	1.62	1.96
Maximum deviation in Mach number	±0.02	±0.01	±0.02
Maximum deviation in stream angle, deg	±0.25	±0.20	±0.20
Average Reynolds number (based on $\bar{c}$ of delta wing)	4.0×10^6	3.5×10^6	3.2×10^6

Accuracy and Limitation of Data

An estimate of the probable errors introduced in the present data by instrument-reading errors and measuring-equipment errors are presented in the following table:

C_L	±0.006
C_l	0.0008
C_m	0.002
C_D	0.003
C_h (balanced control)	0.02
C_h (unbalanced control)	0.01
α, deg	0.1
δ, deg	0.2

The error in δ is the estimated error in the no-load control setting. Corrections for the change in deflection due to control hinge moments were determined from static hinge-moment calibrations and applied to the measured no-load control setting.

Corrections are not available for the transonic nozzle to allow for jet-boundary interference and blockage at transonic speeds or for reflection-plane effects at high subsonic speeds. Furthermore, reflection of the model shock and expansion waves back onto the model by the tunnel walls may appreciably affect the model loadings due to angle of attack at low supersonic Mach numbers but should not appreciably affect the loading due to control deflection. In the fixed Mach number nozzles ($M = 1.41$ and higher), the models were clear of reflected disturbances.

Comparisons of experimental results obtained in the blowdown-tunnel transonic nozzle with those obtained in other facilities (refs. 1 and 9) have served to define the limitations on the usefulness of the present transonic data and to indicate the magnitudes of some of the boundary interference effects. The comparisons have indicated generally satisfactory agreement for the wing and control characteristics due to angle of attack except at Mach numbers between 0.94 and 1.04. The control characteristics due to control deflection, however, are believed reliable throughout the Mach number range. For detailed discussion see references 1 and 9.

RESULTS AND DISCUSSION

The aerodynamic characteristics including hinge-moment coefficients are presented in figure 4 for the unbalanced, unswept control configuration at $M = 0.75$ and are representative of the quality of the basic data obtained in this investigation. Figure 5 presents plots against deflection of the rolling-moment coefficients and the increments in lift and pitching-moment coefficient due to deflection of the unbalanced control for Mach numbers from 0.75 to 1.96. Test data were obtained at positive control deflections for both positive and negative angles of attack. In figure 5 and in subsequent figures the signs of the test values of angle of attack, control deflection, and model force and moment coefficients obtained at negative angles of attack have been arbitrarily reversed for convenience of presentation. This was permissible by reason of model symmetry. Incremental drag coefficients, obtained by subtraction of the zero lift drag at zero deflection, are shown in figure 6 and hinge-moment coefficients in figure 7 as functions of control deflection for the unbalanced control. For the overhang-balanced, swept hinge-line control, incremental values of gross rolling-moment, lift and pitching-moment coefficients, incremental drag coefficients, and hinge-moment coefficients are presented in figures 8, 9, and 10, respectively, as functions of control deflection at Mach numbers from 0.75 to 1.96.

No corrections are available to allow for reflection-plane interference at subsonic and low supersonic Mach numbers. Some error in the absolute values of C_l, ΔC_L, and ΔC_h indicated for differentially deflected ailerons, consequently, is introduced for Mach numbers below 1.09. The error in differences of comparative values, however, is believed small.

Control Effectiveness

For the overhang-balanced, swept hinge-line control values of C_l, ΔC_L, and ΔC_m increased in magnitude with increasing deflection at all

Mach numbers throughout the angle-of-attack and deflection range of the tests (fig. 8). Some loss of effectiveness, as indicated by the reduced slope of the curves C_{l_δ}, ΔC_{L_δ}, and ΔC_{m_δ}, was shown particularly for increasing positive deflections. This is in marked contrast with results shown previously for overhang-balanced controls (see refs. 1 and 2). At subsonic speeds, such controls have been characterized by severe losses in effectiveness at both positive and negative deflections when the control unported (control nose no longer shielded from the airstream by the wing). In references 1 and 2 the unswept constant-chord balanced controls on a 60° delta wing produced little or no changes in wing lift or pitching moment with increasing positive deflections above the unporting angle. Similar effects have been shown for an untapered overhang-balanced, swept hinge-line control on a 45° sweptback wing (ref. 10). The loss of effectiveness has been attributed to reduction of the high peak pressures inherent in the loading at the nose of the control by separation over the wing upper surface when the control unports. In the case of the present balanced control, it is believed that the tapered nose overhang served to greatly decrease these effects through the gradual unporting of the control along the span. At supersonic speeds, the overhang-balanced control of reference 1 showed considerable loss of effectiveness at positive deflection with increasing angle of attack. Although somewhat similar effects are shown for the present control they are apparently greatly attenuated by the overhang taper and perhaps the sweepback of the control nose and hinge line. In general, reduction in curve slopes with increasing angle of attack was shown only at positive deflections, whereas at negative deflections little change may be noted (fig. 8). This dissymmetry of the curves about zero deflection is apparently attributable to decreased losses due to separation when the nose overhang projects on the wing high-pressure side. Similar effects have been noted in reference 1 for the balanced control on a 60° delta wing.

The unbalanced control also maintained effectiveness throughout the Mach number and angle-of-attack and deflection ranges of the tests (fig. 5). In general, the magnitude of values of the curve slopes C_{l_δ}, ΔC_{L_δ}, and ΔC_{m_δ} decreased somewhat with either increasing angle of attack or deflection at deflections greater than 10°. The changes in curve-slope values with changes in angle of attack and deflection were most pronounced at transonic Mach numbers near 1.0.

Figure 11 shows the variation with Mach number of the slope values of the curves of C_l, ΔC_L, and ΔC_m against deflection (measured perpendicular to the hinge line) taken at zero angle of attack and deflection for both controls. Comparison of the magnitude of the slope parameters for the two controls cannot be made in a quantitative sense because of the differences in control size and wing plan forms (see fig. 1);

however, the moment areas of the two controls about both the rolling-moment reference axis and the pitching-moment reference axis were approximately equal. Figure 11(b) shows that although the effectiveness parameters were smaller for the balanced control than for the unbalanced control, the changes with Mach number were not greatly different except near $M = 1.0$. In the transonic range the smaller changes shown for the balanced control may be attributable to the bluntness of the control trailing edge. Comparison of experiment with calculations based on the method of reference 11 (and ignoring carryover effects on fuselage behind wing) shows that at supersonic speeds C_{l_δ} for the unbalanced control was about 80 percent of that predicted by theory, whereas C_{L_δ} was underestimated approximately 10 percent by theory. Estimates, based on linear theory, for the balanced control were made only for $M = 1.96$ (the control leading edge was swept behind the Mach line at lower Mach numbers) and indicated values of C_{l_δ} and C_{L_δ} of the same order as the theoretical values for the unbalanced control. The measured values, consequently, were about 50 percent of the predicted value.

Control Hinge Moments

For the overhang-balanced control, hinge-moment coefficients due to deflection were small at Mach numbers below 1.0 (fig. 10). At $M = 0.75$, the control was slightly overbalanced (positive change in coefficient with increasing angle). With increasing Mach number, the slopes of the curves changed in a negative (unbalancing) direction throughout the transonic speed range. The hinge-moment variations with deflection, at subsonic speeds, were moderate and much less nonlinear than those previously shown for unswept overhang-balanced controls (refs. 1 and 2). For these controls or a swept back overhang-balanced control (ref. 10), at subsonic and transonic speeds, the loss in lift effectiveness when the control unported has been accompanied by severe unbalancing changes in slope of the hinge-moment curves. Such behavior was not shown for the balanced control of the present report. In fact, an increase in balancing effectiveness (positive change in curve slope) occurred at about the deflection at which the inboard end of the control unported. This increase may be attributable to tip losses decreasing the overall control loading behind the hinge line and thereby reducing the unbalancing moment. At higher deflections the expected loss in balancing effectiveness apparently was minimized by the gradual unporting of the control along the span. At supersonic speeds, some loss in hinge-moment-balancing effectiveness of the overhang-balance area was shown for small deflections. At higher deflections, as the control began to unport, the overhang became increasingly effective. Angle of attack had only small effects on the hinge-moment coefficients of the balanced control at subsonic Mach numbers. At supersonic speeds, the negative

increase in hinge-moment coefficients with increasing angle of attack was considerably greater at negative deflections than at positive deflections and apparently resulted from increased effectiveness of the nose overhang when projecting on the wing high-pressure side.

For the unbalanced control the variations of hinge-moment coefficient with deflection exhibited no serious nonlinearities except possibly at $M = 0.75$ (fig. 7). The curves, which had negative slope values at all Mach numbers, were displaced negatively but otherwise not appreciably affected by angle of attack.

Comparison of the hinge-moment data for the two controls indicates that the increment in hinge moment associated with the rearward and outward movement of the control center of pressure at transonic speeds was greatly reduced by the hinge-line sweepback of the balanced control. This is shown in figure 11(a) by the control parameters $C_{h_\alpha}\left(\frac{M_a}{M_{a_1}}\right)$ and $C_{h_\delta}\left(\frac{M_a}{M_{a_1}}\right)$ taken at $\alpha = 0^\circ$ and $\delta = 0^\circ$. In figure 11(a) comparison is made of the hinge-moment coefficients reduced on the basis of the moment area of the control about the control leading edge. This affords comparison of the actual hinge moments for the two controls on a more nearly equal basis. Values of C_{h_δ} for the balanced control were near zero at subsonic speeds and increased much less rapidly at transonic speeds than for the unbalanced control. The smaller increase in hinge moments is attributed to the hinge-line sweepback of the balanced control since, in general, the simple addition of control balance area has not reduced the change in hinge moment with Mach number at transonic speeds (see refs. 1, 2, 3, and 10). For the balanced control C_{h_δ} reached a maximum at about $M = 1.25$, a value approximately 20 percent of that of the unbalanced control, and was constant to higher Mach numbers. Similarly, C_{h_α} for the balanced control increased slowly at transonic speeds and reached a maximum at about the same Mach number, a value about 33 percent of that of the unbalanced control. At higher supersonic Mach numbers the balanced control lost much of its advantage because of the decrease in C_{h_δ}, for the unbalanced control, with increasing Mach number.

Control Drag

Zero-lift drag values have little value, principally because of the presence of the boundary-layer shim on the test body and have therefore been subtracted from all drag coefficients presented in figures 6 and 9. The values of the incremental drag coefficients due to angle of

attack are of questionable reliability at transonic speeds because of boundary interference effects (see ref. 9); the drag-coefficient increments due to control deflection, however, were believed to have been unaffected. Comparison of figures 6 and 9 shows that the drag coefficient generally increased more rapidly with deflection for the unbalanced control than for the balanced control. This is illustrated in figure 12 by the variation with Mach number of the increment in drag coefficient due to two oppositely deflected ailerons. A 10° deflection was chosen for comparison of the unbalanced and balanced controls. The figure shows that ΔC_D for the balanced control was little more than half that for the unbalanced control at $\alpha = 0^\circ$ and at $\alpha = 8^\circ$ was less than half the value for the unbalanced control at transonic speeds although this value increased to 70 percent at $M = 1.96$.

Evaluation of Control Characteristics

In order to evaluate the characteristics of the two controls under practical conditions, figures 13 and 14 are presented. The upper plot of figure 13 presents values of C_l estimated to be required to produce an arbitrary roll rate of 15 radians per second for both wings at an altitude of 40,000 feet for an assumed wing area of 204.2 square feet (the areas of a single aileron in terms of this figure were 3.8 and 4.9 percent for the unbalanced and balanced control, respectively). Because of the low values of C_{l_p} for such a highly swept wing, values of C_l estimated for a lower rate of roll and a smaller wing size, more practical for a missile, were too small at supersonic speeds to permit reasonable accuracy in reading the experimental data plots. The values of C_l were calculated by use of theoretical values of C_{l_p} from references 12 and 13. Although the values of C_l do not account for effects of wing twist on aileron effectiveness, effects of angle of attack on C_{l_p}, and other factors that may be of importance in practice, their variations with Mach number should be fairly typical if a constant rate of roll is the criterion.

The other two plots of figure 13 show experimental values of hinge-moment coefficient for equal up and down deflection of opposite ailerons which would result from the calculated required rolling moment. The parameter $C_h\left(\frac{M_a}{M_{a_2}}\right)$ is used to afford a direct comparison of the hinge moments of the two controls. Data are shown for the static and steady roll cases. Data for the static case are representative of the condition

in which the ailerons are fully deflected before the aircraft starts to roll. The steady-roll case is included to give an indication of the balancing effects on aileron hinge moments due to rolling which occur when values of C_{h_α} are negative. The aileron hinge-moment coefficients for the steady-roll case were determined by computing the induced angle of attack at the aileron centroid and assuming the effective angle of attack to be the initial angle of attack plus this induced angle. It should be mentioned that although induced angle of attack is a direct function of the value of $\frac{pb}{2V}$, for a given wing-aileron configuration, the relation between the hinge moment due to angle of attack and the hinge moments due to deflection is very nearly independent of the value of $\frac{pb}{2V}$. That is, if linearity of the variations of hinge moment and rolling moment with α and δ were assumed, then the hinge moments for the steady-roll case in percent of the hinge moments for the static case would be unchanged by reduction in the assumed roll rate or wing size.

Values of the hinge-moment parameters of figure 13 are shown for $\alpha = 0$ and $\alpha = 8^\circ$ for both balanced and unbalanced controls. A moderate increase in the parameters for the balanced control is shown at transonic speeds followed by a less rapid increase at supersonic speeds, whereas for the unbalanced control the parameter increased rapidly with Mach number at transonic speeds then decreased above $M = 1.25$. These data indicate much smaller hinge moments for the balanced control at transonic and small supersonic Mach numbers and support the theoretical analysis of reference 14, which showed that for a low-aspect-ratio control, a highly swept hinge line would minimize control hinge moments. For the smaller hinge moments correspondingly less torque would be required to be available at the control and the strength and weight of the actuating mechanism could be reduced. The advantages to the balanced control, however, decreased at the higher Mach numbers but were still considerable at 8° angle of attack. The differences in hinge moments between the two controls were not as great for the steady roll case as for the static case because of the larger values of C_{h_α} of the unbalanced control.

The work required to overcome the hinge moments due to deflection is an important consideration since it determines the amount of energy which must be supplied to the power-boost system. A comparison on the basis of deflection work for the two controls producing the above roll rate is presented in figure 14 at angles of attack of 0° and 8°. These data indicate that the deflection work was appreciably less for the balanced control than for the unbalanced control at subsonic and transonic speeds; at high supersonic speeds, however, the differences were small for

both the static case and steady-roll case. This came about because of the increased deflection of the balanced control required to produce the above roll rate.

Estimates of the effect of control size on the presented comparisons indicated that reduction in area of the balanced control to that of the area of the unbalanced control would not change the values of the hinge-moment parameter. The values of deflection work, however, would be increased approximately 40 percent because of the increase in the required deflection.

CONCLUSIONS

An investigation of an 80° swept pointed wing with an unbalanced constant-chord control and an overhang-balanced swept hinge-line control in the Langley 9- by 12-inch blowdown tunnel at Mach numbers from 0.75 to 1.96 indicated the following conclusions:

1. Both controls were effective throughout the range of the investigation including angles of attack of ±16° and control deflections of 25°. Although the balanced control was less effective than the unbalanced control in producing changes in C_l, C_L, and C_m, the decrease in effectiveness from subsonic to high supersonic speeds was of the same order for both controls.

2. The tapered overhang of the balanced swept hinge-line control effectively balanced the control hinge moments at subsonic speeds without introducing severe nonlinearities in the variations with deflections of hinge moment, lift, and rolling moment such as have been shown previously for unswept untapered overhang-balanced controls.

3. Comparison of the hinge-moment characteristics for the balanced and unbalanced controls indicated that the increment in hinge moment associated with the rearward and outward movement of the center of pressure at transonic speeds was greatly reduced by the hinge-line sweepback of the balanced control. At supersonic speeds the hinge moments due to deflection were from 20 to 33 percent of those of the unbalanced control.

4. With the control deflected to produce a given roll rate the magnitude of the hinge moments for the balanced control, up to moderate angles of attack, showed less change with Mach number at transonic speeds and were much smaller at small supersonic Mach numbers than for the unbalanced control. At the highest Mach number, however, the differences in hinge moments were not great.

5. Comparison of the two controls on the basis of deflection work for the same roll rate showed only slight advantage to the balanced control at supersonic speeds because of the large required control deflections.

Langley Aeronautical Laboratory,
National Advisory Committee for Aeronautics,
Langley Field, Va., May 21, 1956.

REFERENCES

1. Guy, Lawrence D.: Effects of Overhang Balance on the Hinge-Moment and Effectiveness Characteristics of an Unswept Trailing-Edge Control on a 60° Delta Wing at Transonic and Supersonic Speeds. NACA RM L54G12a, 1954.

2. Thompson, Robert F.: Hinge-Moment, Lift, and Pitching-Moment Characteristics of a Flap-Type Control Surface Having Various Hinge-Line Locations on a 4-Percent-Thick 60° Delta Wing - Transonic-Bump Method. NACA RM L54B08, 1954.

3. Guy, Lawrence D.: Control Hinge-Moments and Effectiveness Characteristics of a Horn-Balanced, Flap-Type Control on a 55° Sweptback Triangular Wing of Aspect Ratio 3.5 at Mach Numbers of 1.41, 1.62, and 1.96. NACA RM L52L15, 1953.

4. Davis, Don D., Jr., and Hieser, Gerald: Loads on Thin Wings at Transonic Speeds. NACA RM L55E11c, 1955.

5. Conner, D. William: Aerodynamic Characteristics of Two All-Movable Wings Tested in the Presence of a Fuselage at a Mach Number of 1.9. NACA RM L8H04, 1948.

6. Mitchell, Meade H., Jr.: Effects of Varying the Size and Location of Trailing-Edge Flap-Type Controls on the Aerodynamic Characteristics of an Unswept Wing at a Mach Number of 1.9. NACA RM L50F08, 1950.

7. Burgess, Warren C., Jr., and Seashore, Ferris L.: Criterions for Condensation-Free Flow in Supersonic Tunnels. NACA TN 2518, 1951.

8. May, Ellery B., Jr.: Investigation of the Effects of Leading-Edge Chord-Extensions on the Aerodynamic and Control Characteristics of Two Sweptback Wings at Mach Numbers of 1.41, 1.62, and 1.96. NACA RM L50L06a, 1951.

9. Guy, Lawrence D., and Hadaway, William M.: Aerodynamic Loads on an External Store Adjacent to a 45° Sweptback Wing at Mach Numbers From 0.70 to 1.96, Including an Evaluation of Techniques Used. NACA RM L55H12, 1955.

10. Lockwood, Vernard E., and Hagerman, John R.: Aerodynamic Characteristics at Transonic Speeds of a Tapered 45° Sweptback Wing of Aspect Ratio 3 Having a Full-Span Flap Type of Control With Overhang Balance. NACA RM L51L11, 1952.

11. Tucker, Warren A., and Nelson, Robert L.: Theoretical Characteristics in Supersonic Flow of Two Types of Control Surfaces on Triangular Wings. NACA Rep. 939, 1949.

12. Polhamus, Edward C.: A Simple Method of Estimating the Subsonic Lift and Damping in Roll of Sweptback Wings. NACA TN 1862, 1949.

13. Malvestuto, Frank S., Jr., Margolis, Kenneth, and Ribner, Herbert S.: Theoretical Lift and Damping in Roll at Supersonic Speeds of Thin Sweptback Tapered Wings With Streamwise Tips, Subsonic Leading Edges, and Supersonic Trailing Edges. NACA Rep. 970, 1950. (Supersedes NACA TN 1860.)

14. Goin, Kennith L.: Theoretical Analyses To Determine Unbalanced Trailing-Edge Controls Having Minimum Hinge Moments Due to Deflection at Supersonic Speeds. NACA TN 3471, 1955. (Supersedes NACA RM L51F19.)

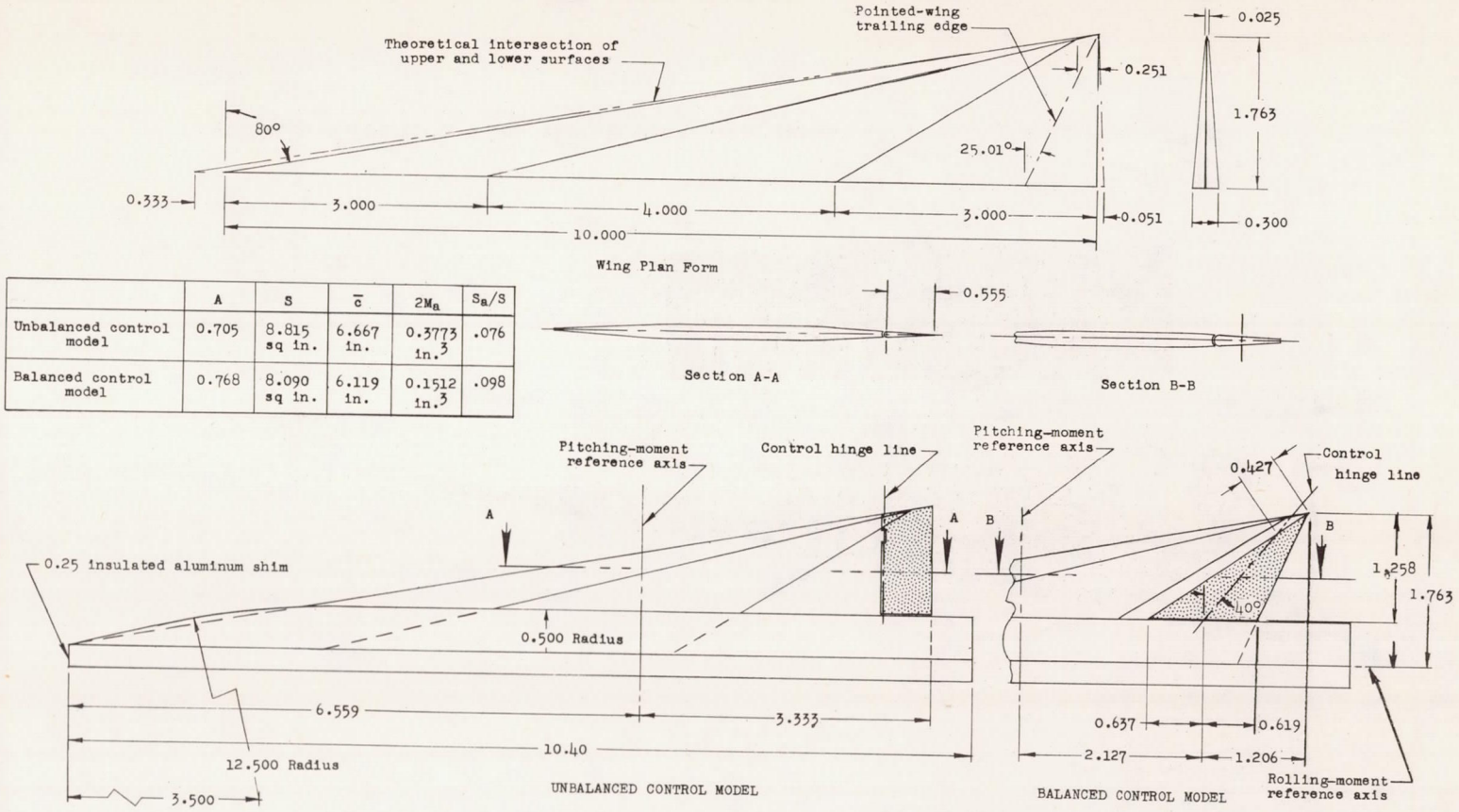

	A	S	$\bar{c}$	$2M_a$	S_a/S
Unbalanced control model	0.705	8.815 sq in.	6.667 in.	0.3773 $in.^3$	.076
Balanced control model	0.768	8.090 sq in.	6.119 in.	0.1512 $in.^3$	.098

Figure 1.- Details of semispan-wing—fuselage combination. All dimensions in inches unless otherwise noted.

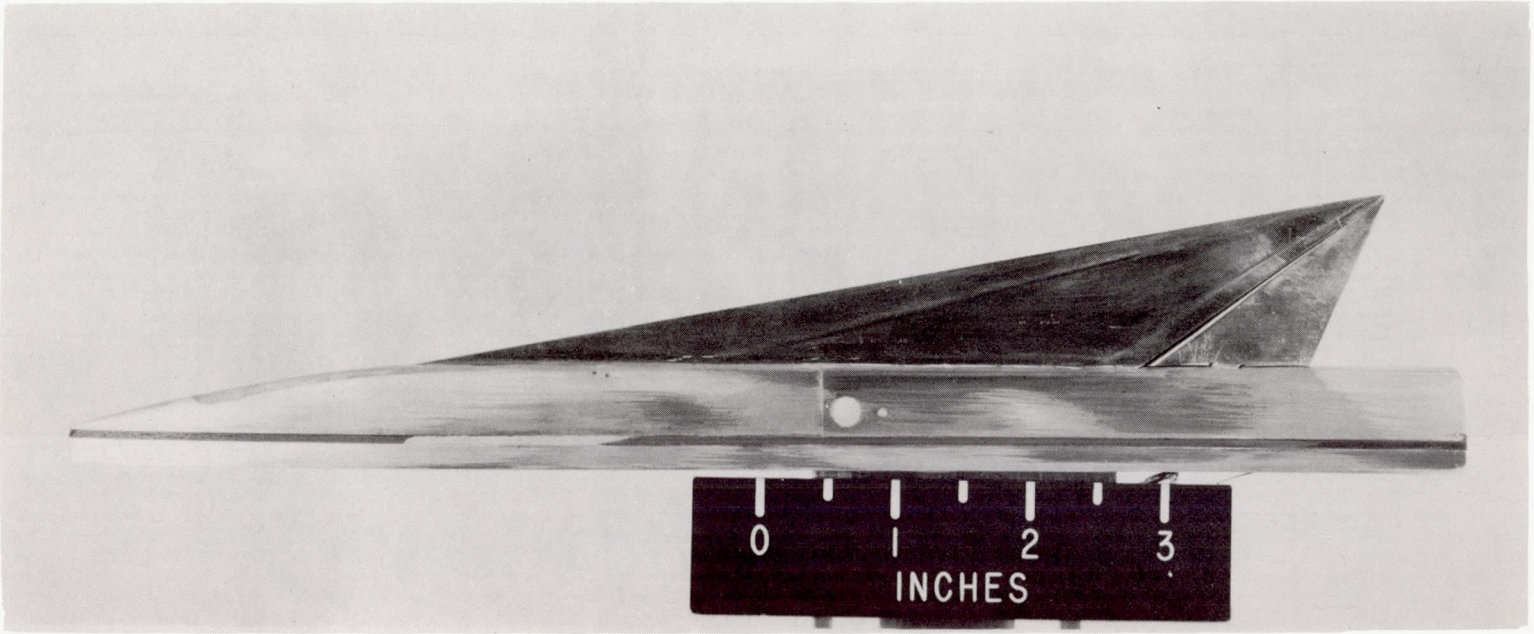

L-80946.1

Figure 2.- Pointed wing model with overhang-balanced, swept hinge-line control.

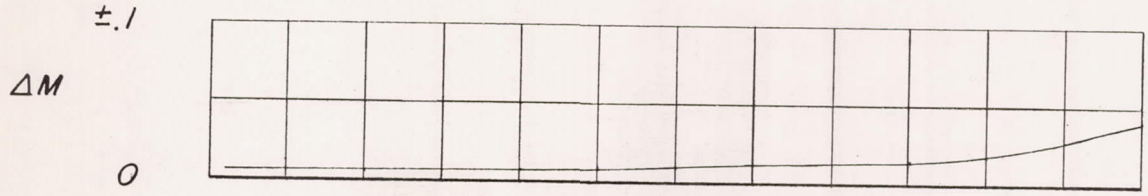

(a) Maximum deviation from average test-section Mach number.

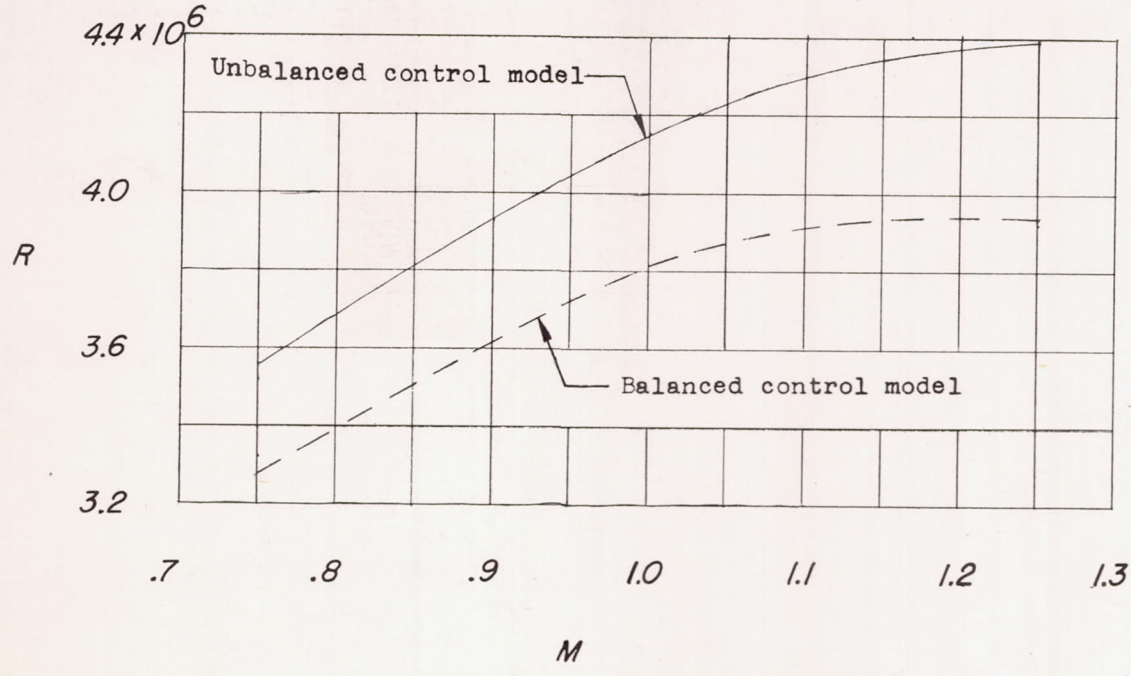

(b) Average test Reynolds number based on wing $\bar{c}$.

Figure 3.- Test-section Mach number and Reynolds number characteristics of the transonic nozzle and model.

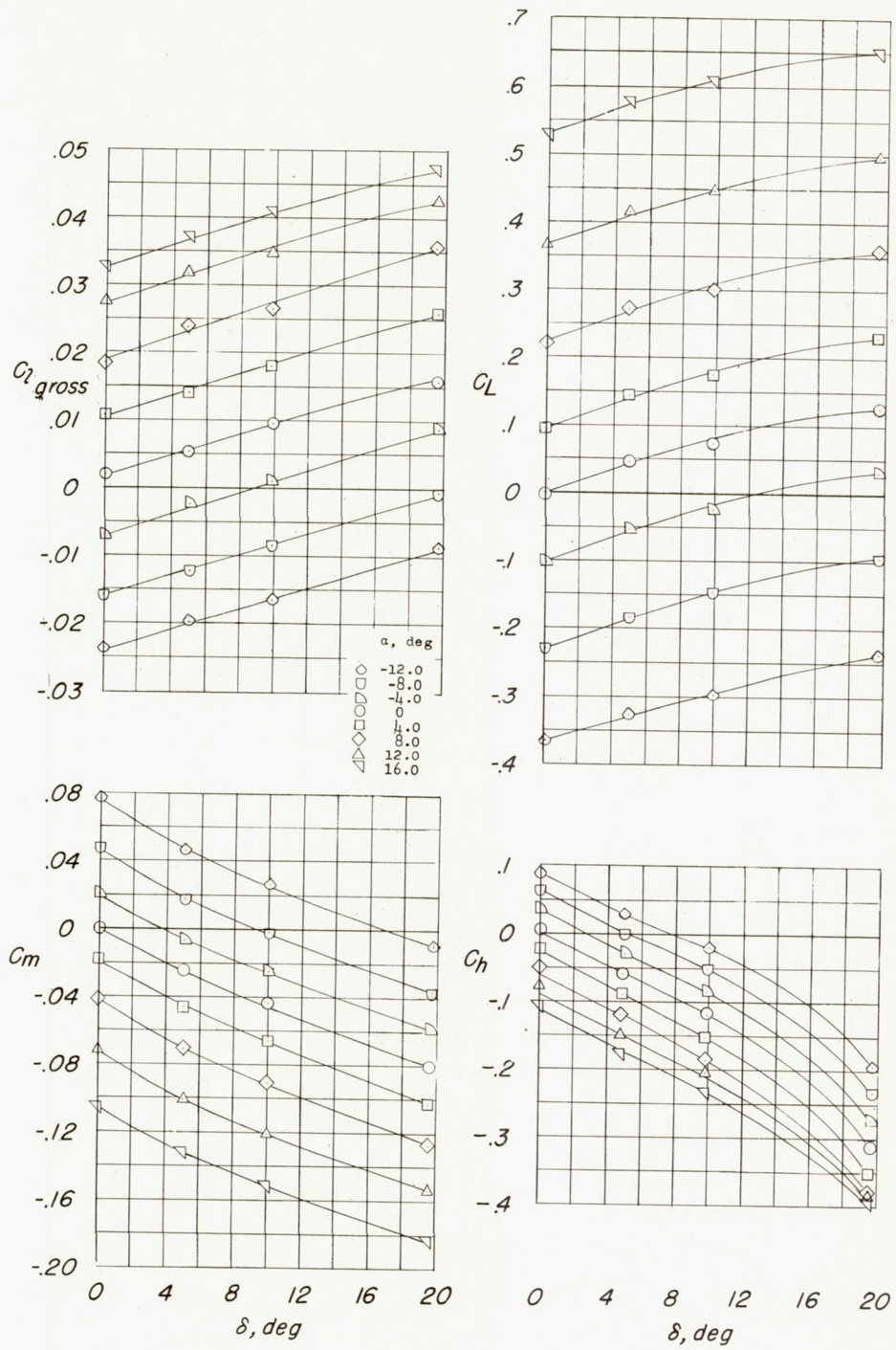

Figure 4.- Aerodynamic characteristic, including hinge-moment coefficients, of combination of fuselage and 80° swept pointed wing. Unbalanced control. M = 0.75.

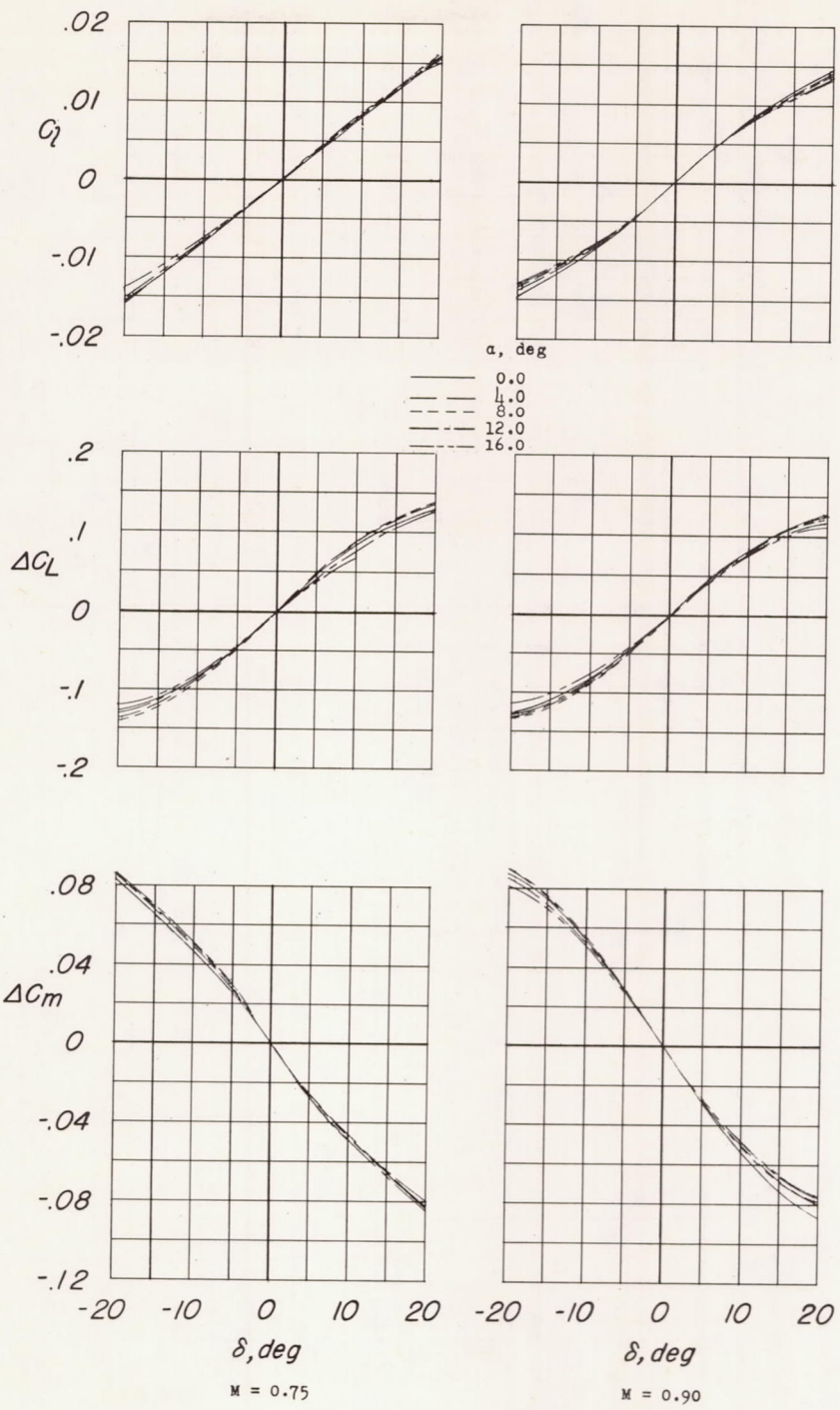

Figure 5.- Variation with control deflection of the rolling-moment and increments of lift and pitching-moment coefficients due to deflection at various angles of attack. Unbalanced control.

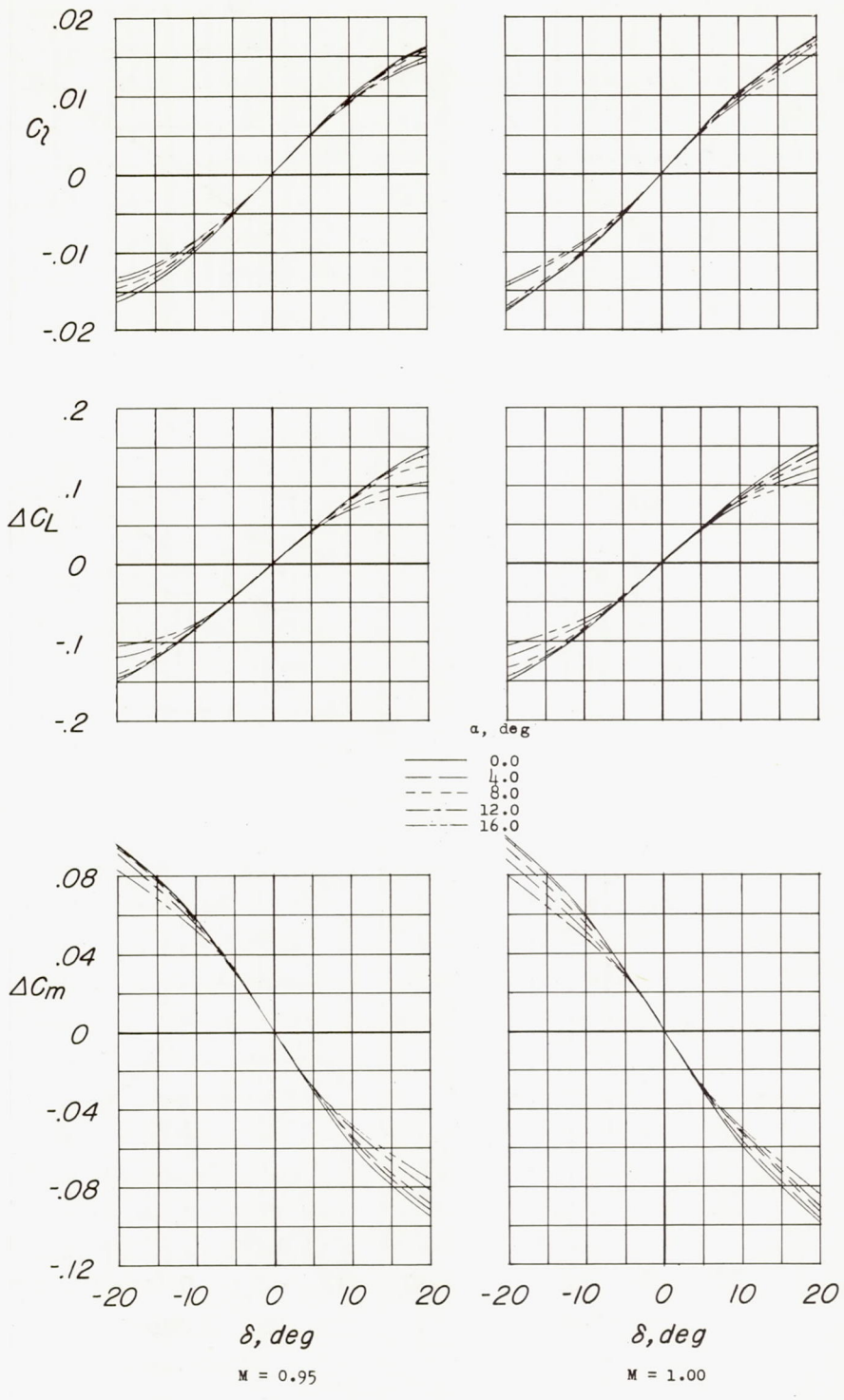

Figure 5.- Continued.

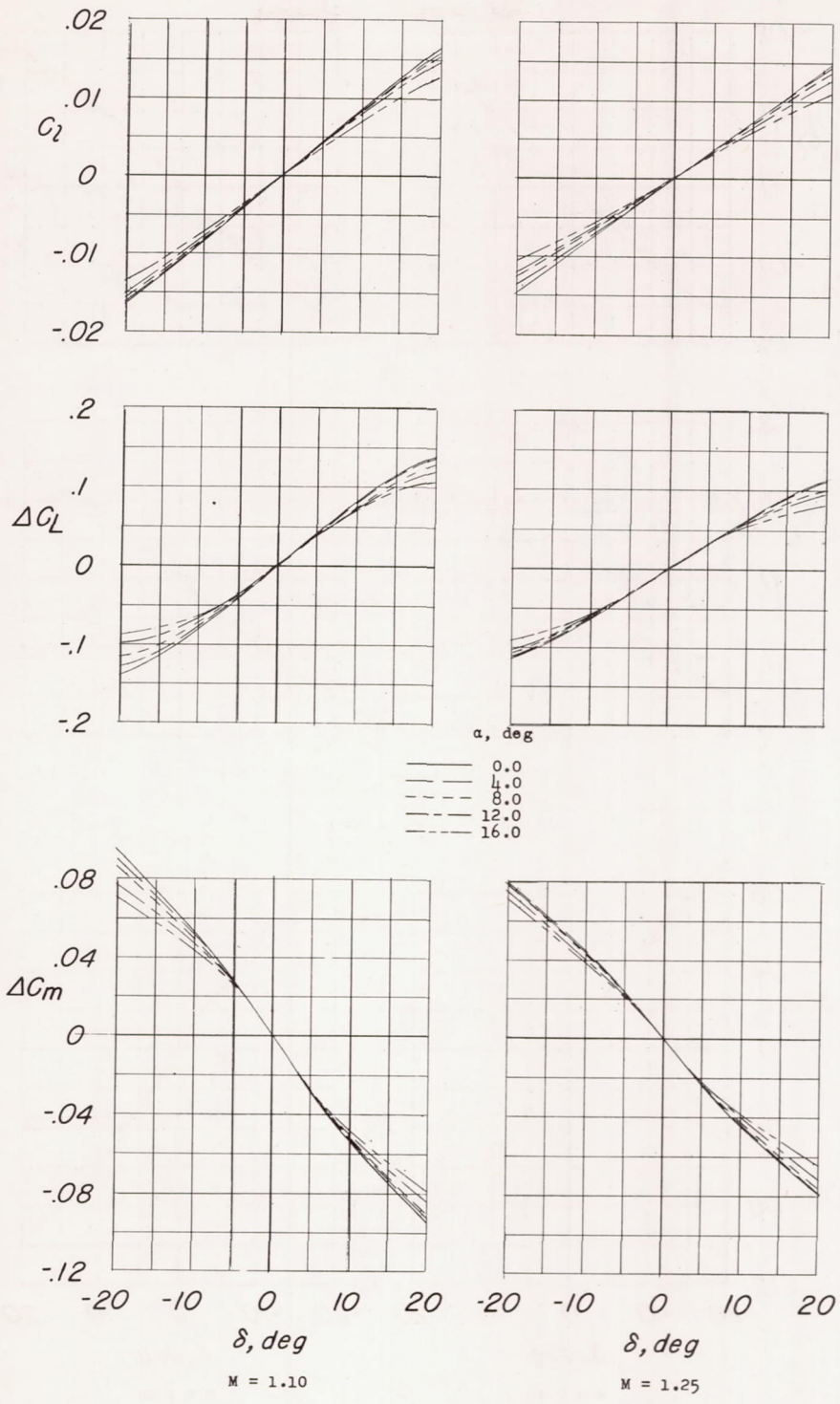

Figure 5.- Continued.

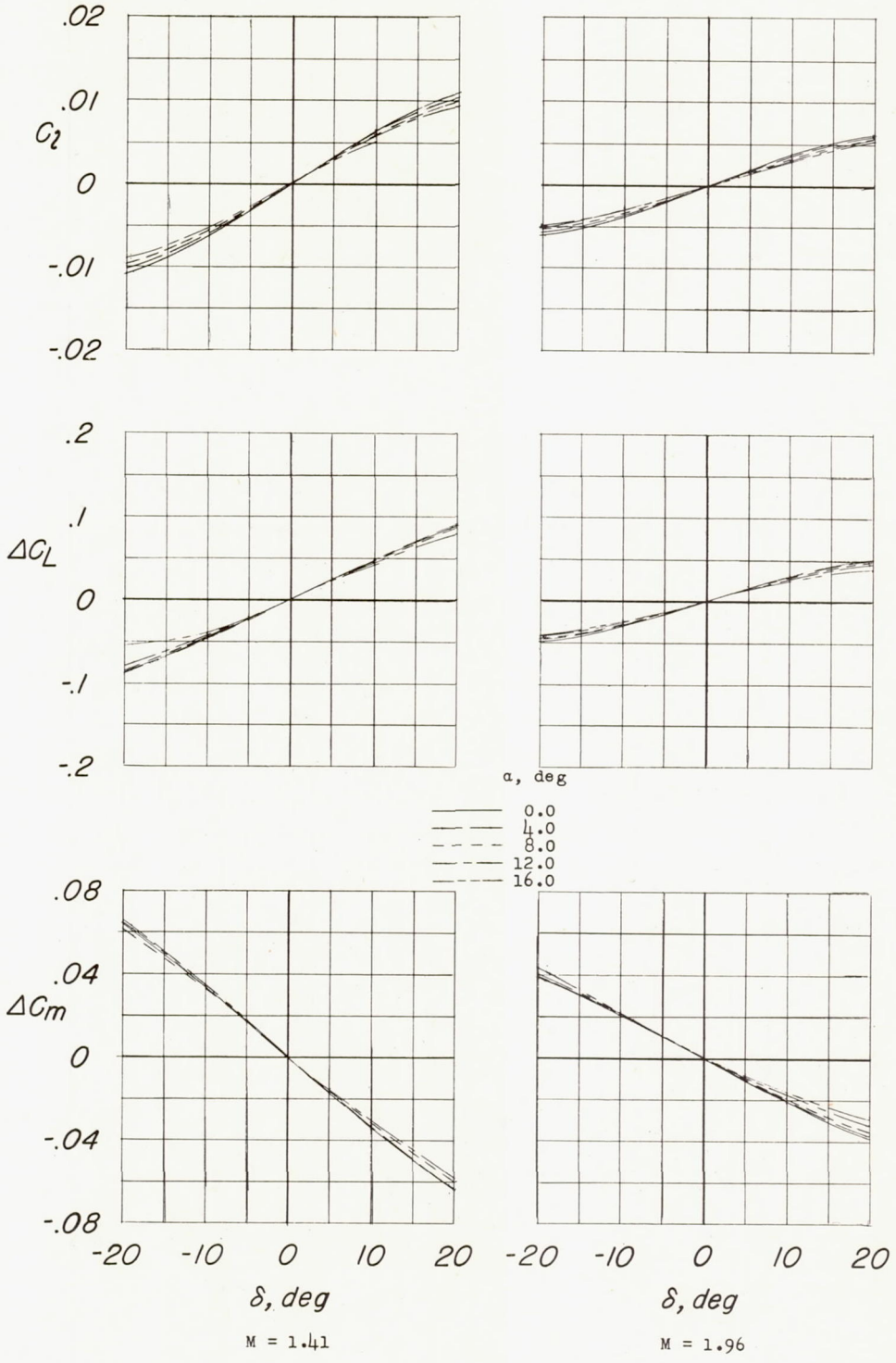

Figure 5.- Concluded.

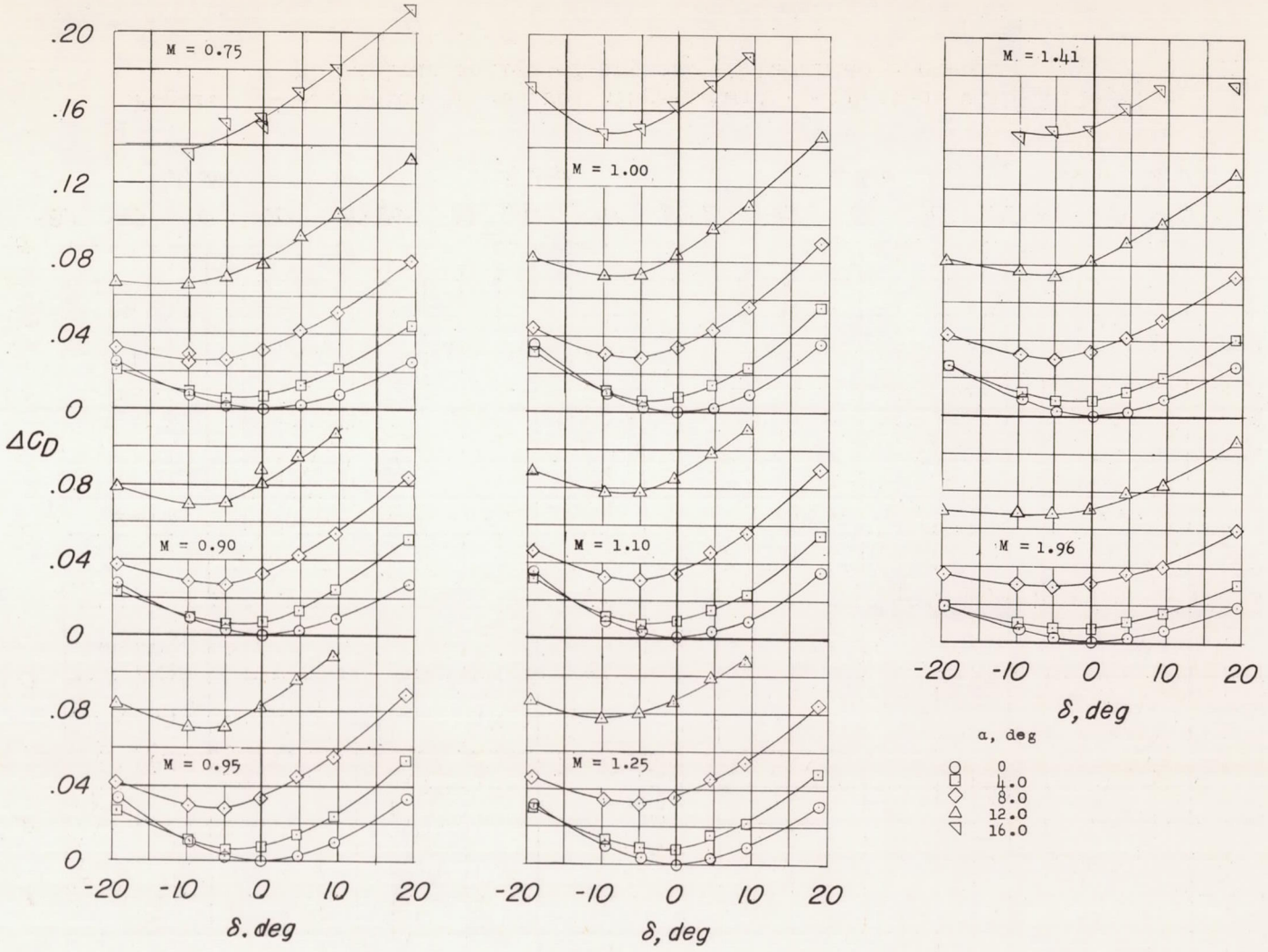

Figure 6.- Variation with control deflection of the increments of drag coefficient due to angle of attack and deflection. Unbalanced control.

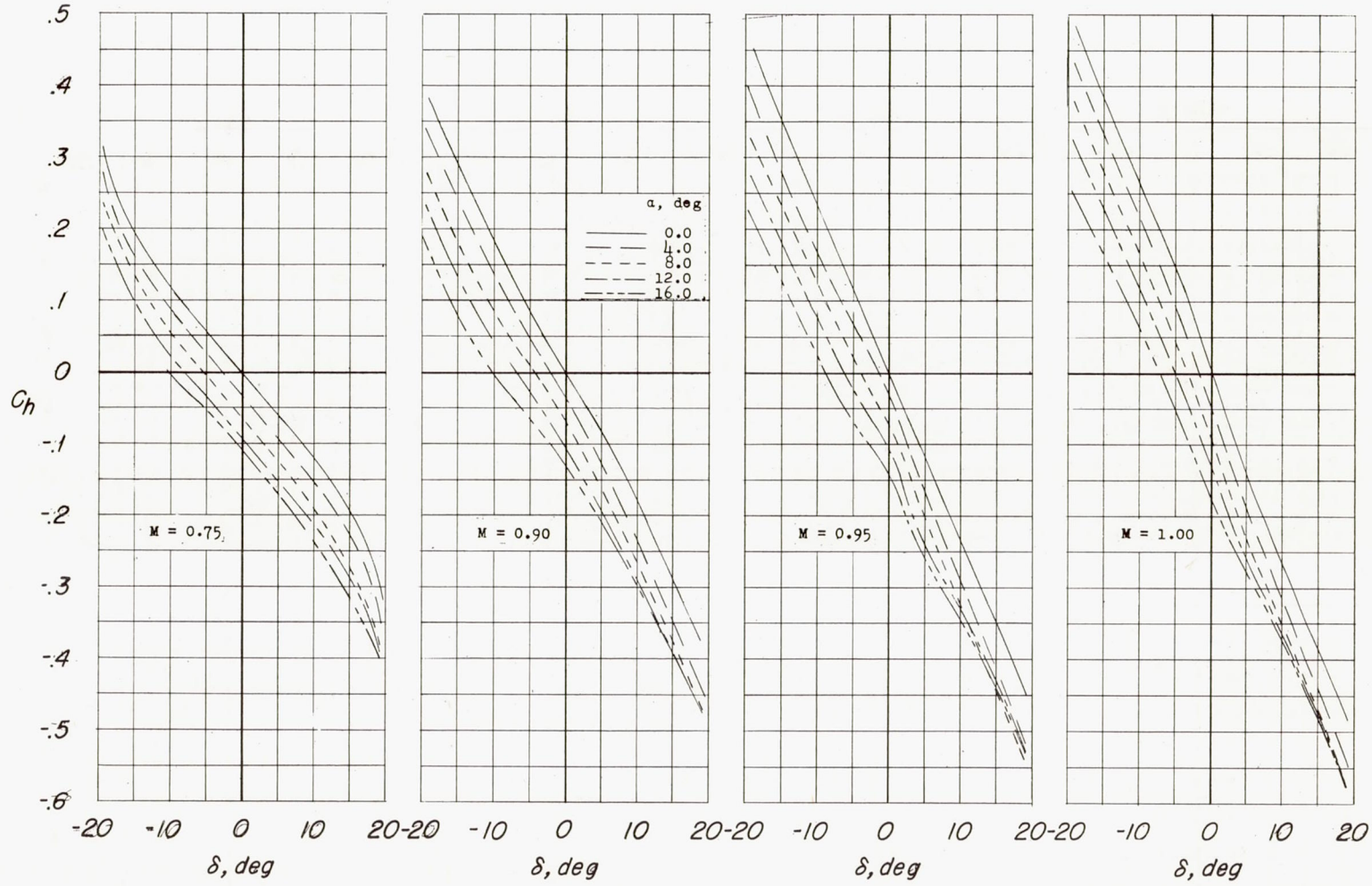

Figure 7.- Variation of control hinge-moment coefficient with deflection at various angles of attack. Unbalanced control.

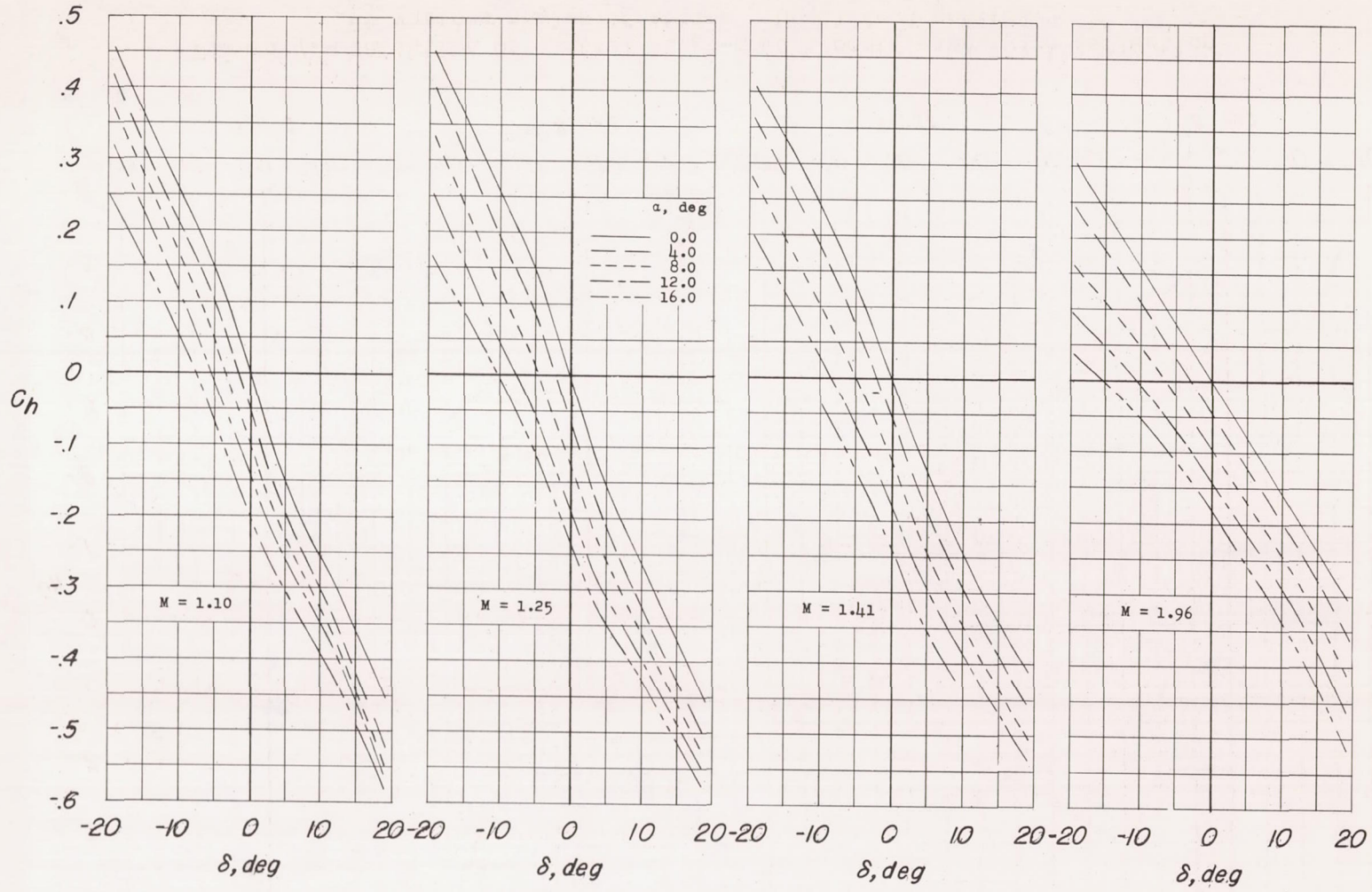

Figure 7.- Concluded.

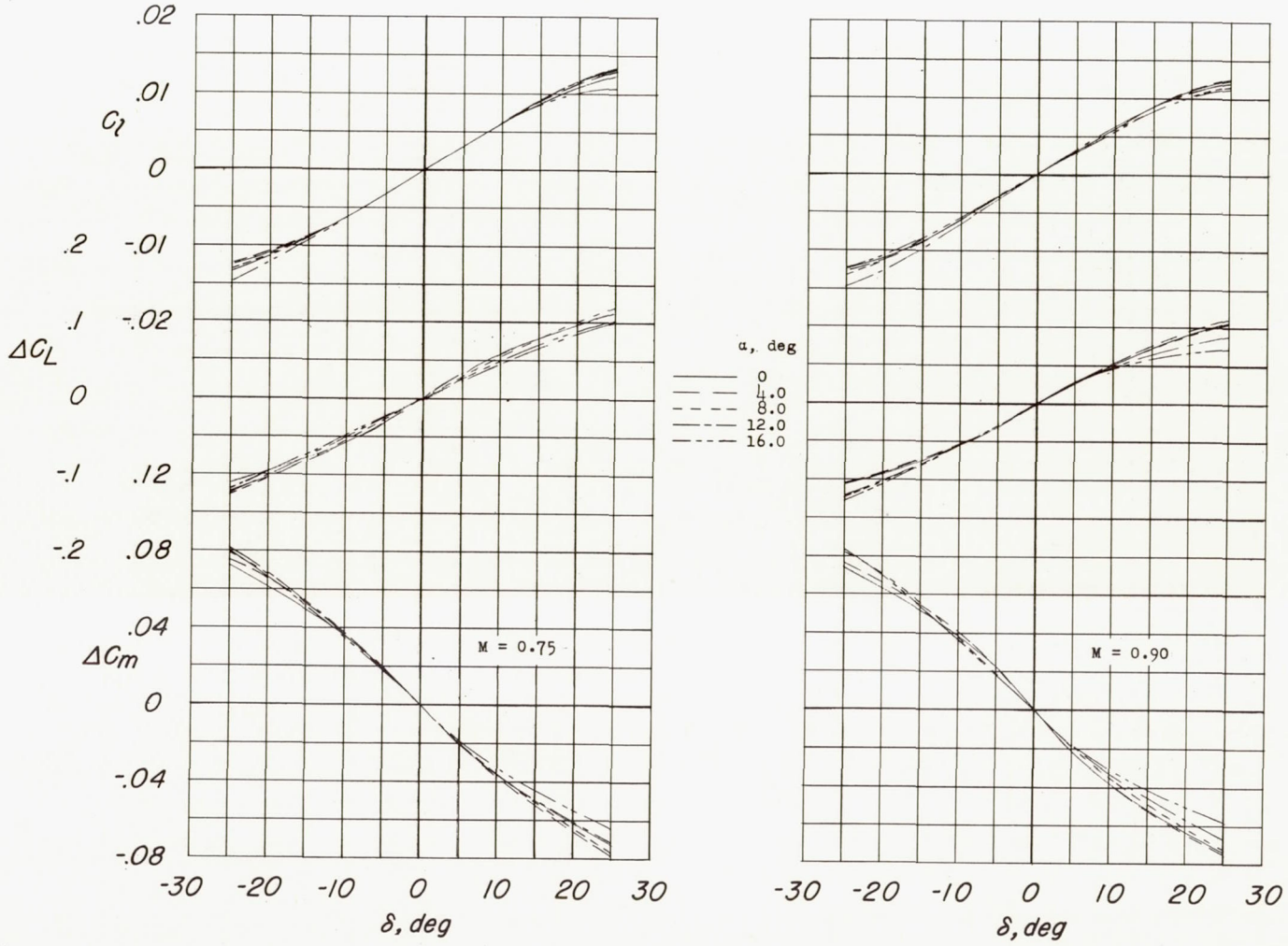

Figure 8.- Variation with control deflection of the rolling moment and increments of lift and pitching-moment coefficients due to deflection at various angles of attack. Balanced control.

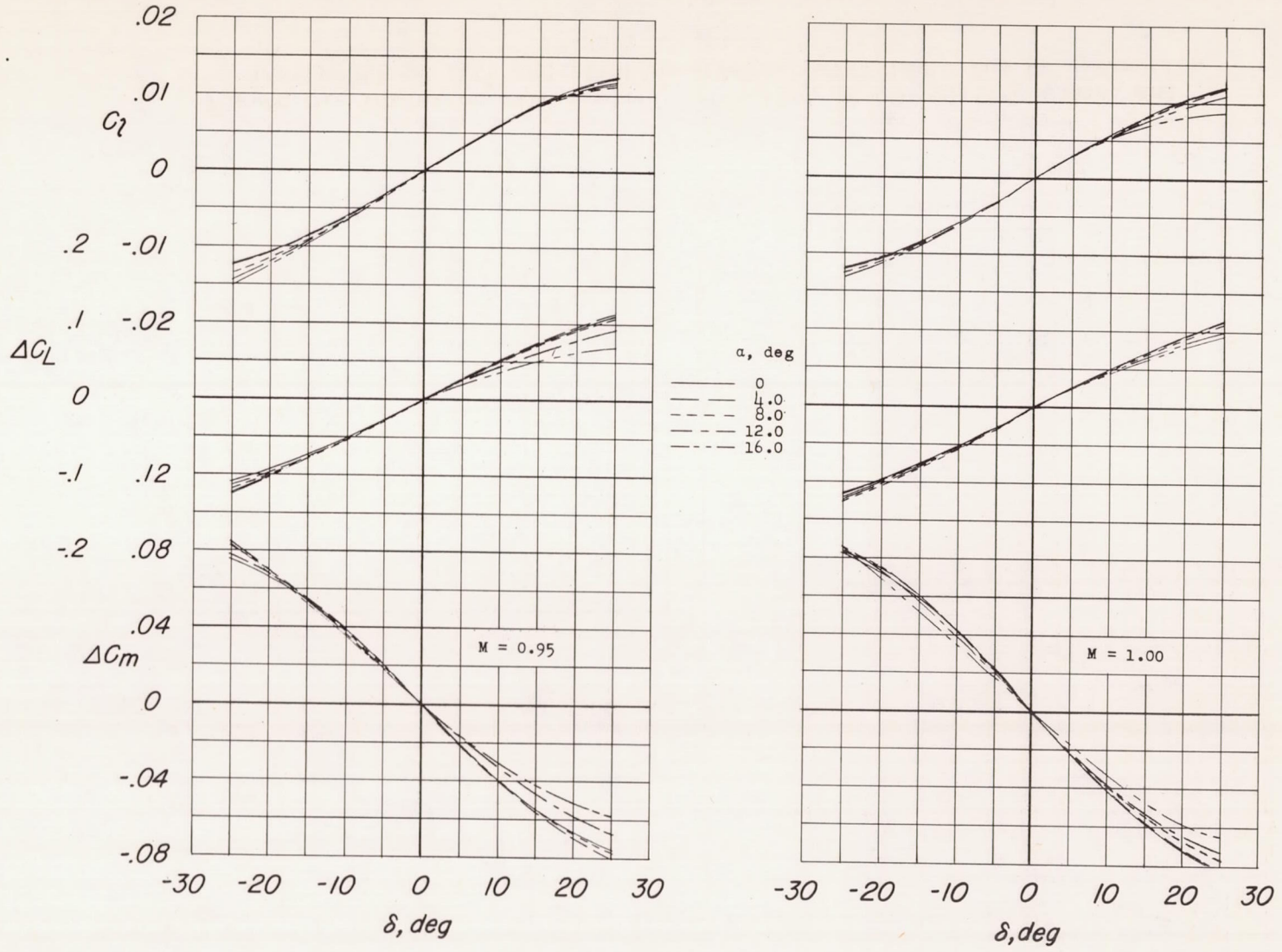

Figure 8.- Continued.

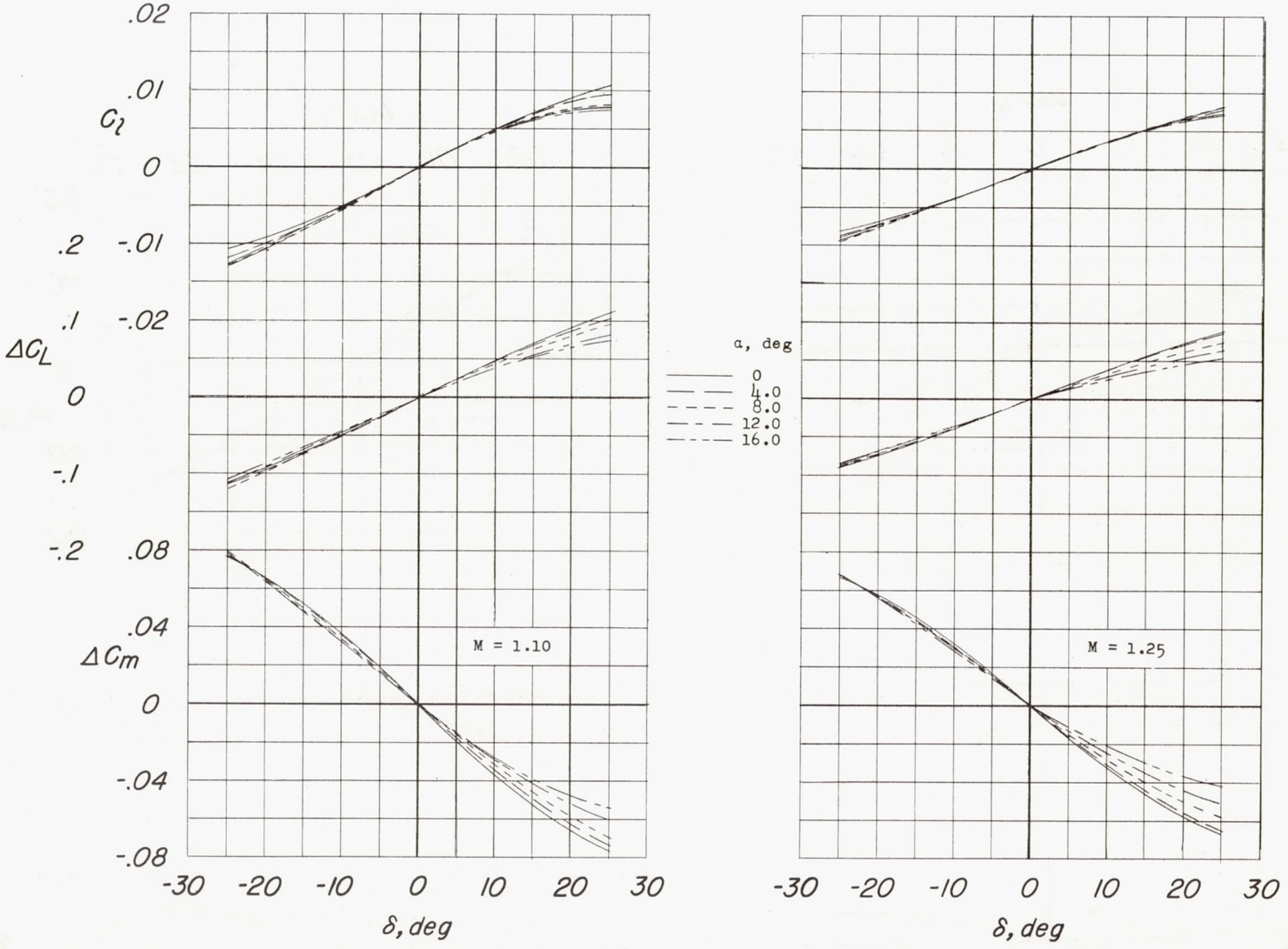

Figure 8.- Continued.

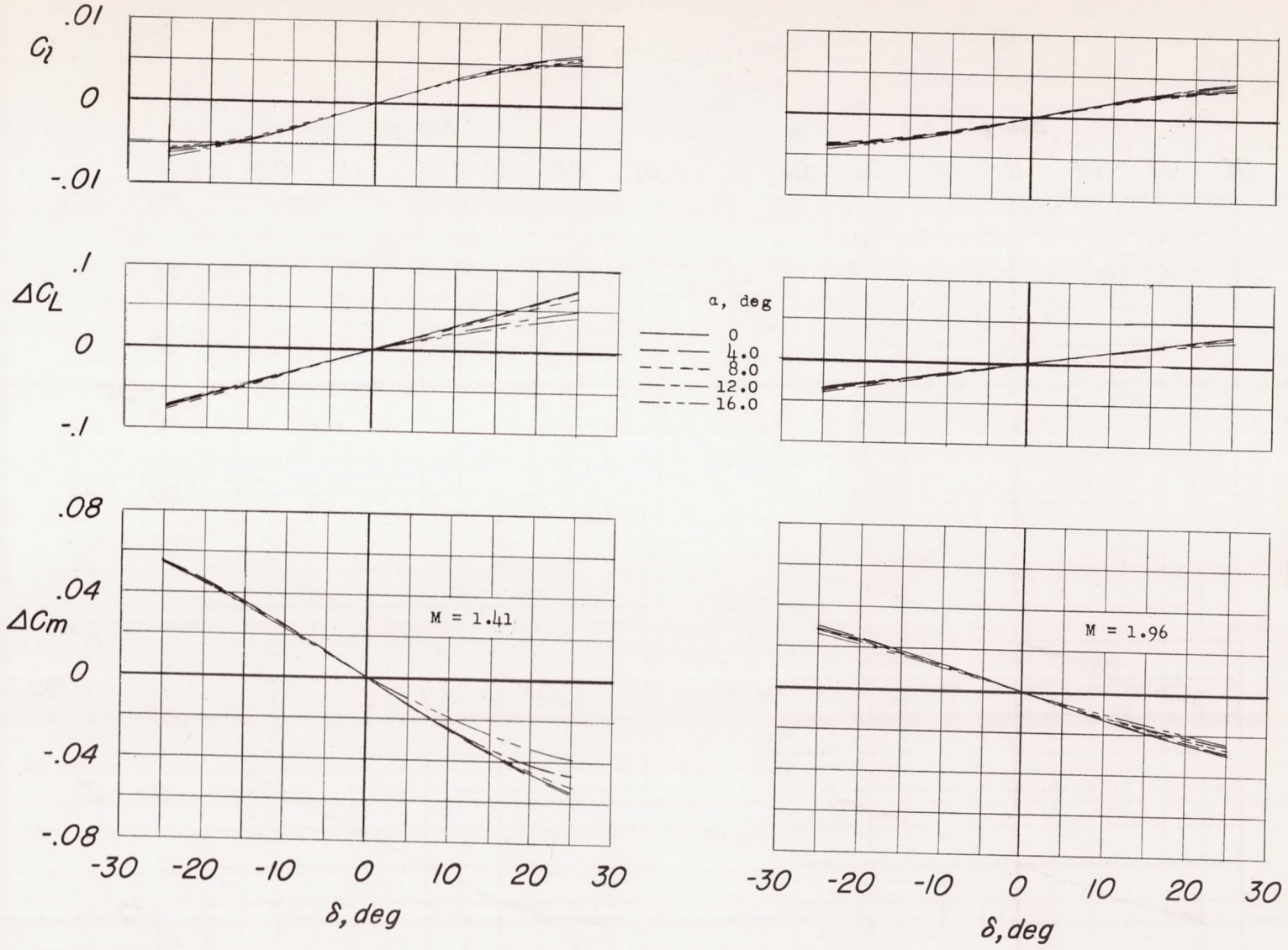

Figure 8.- Concluded.

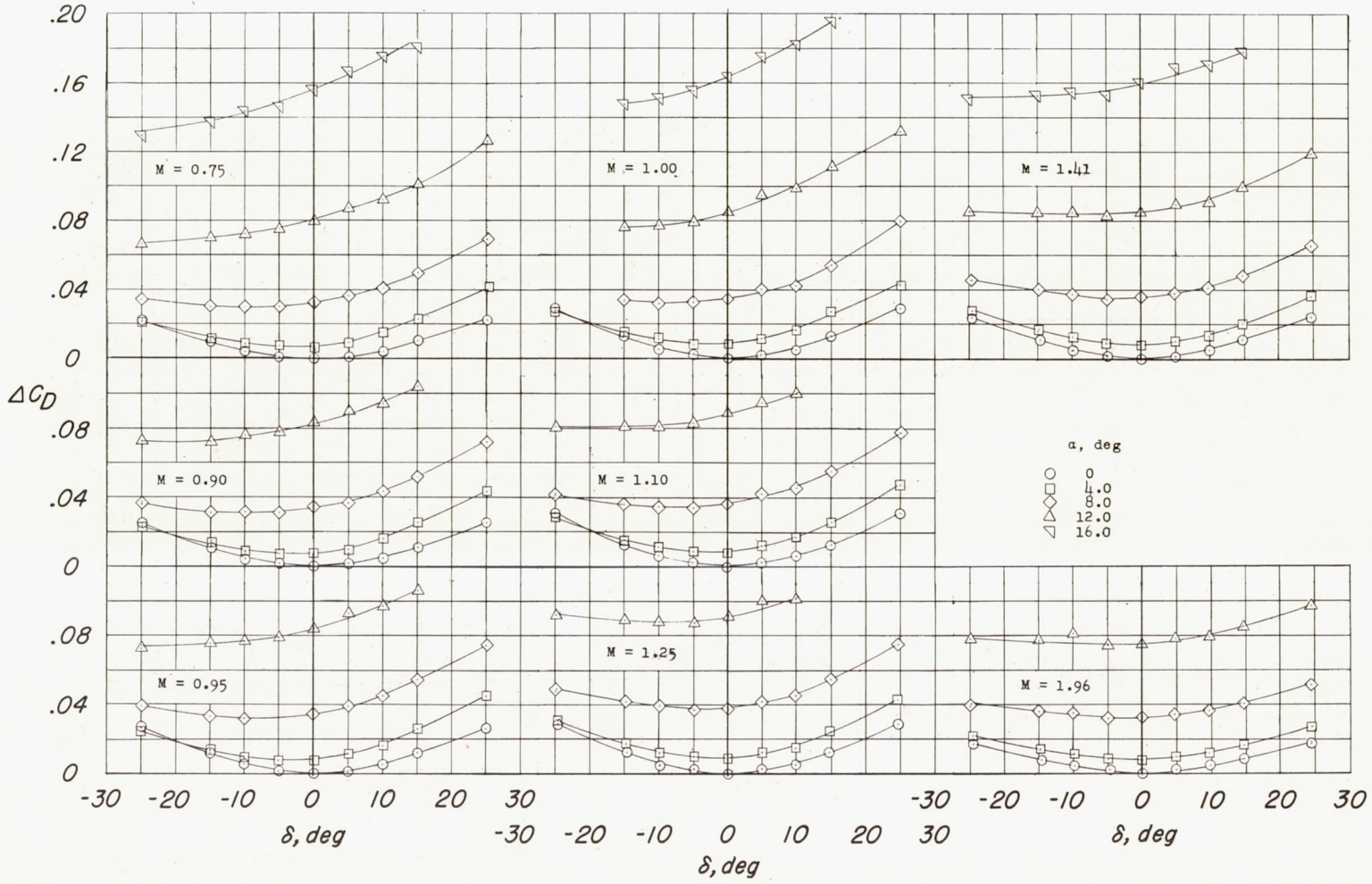

Figure 9.- Variation with control deflection of the increments of drag coefficient due to angle of attack and deflection. Balanced control.

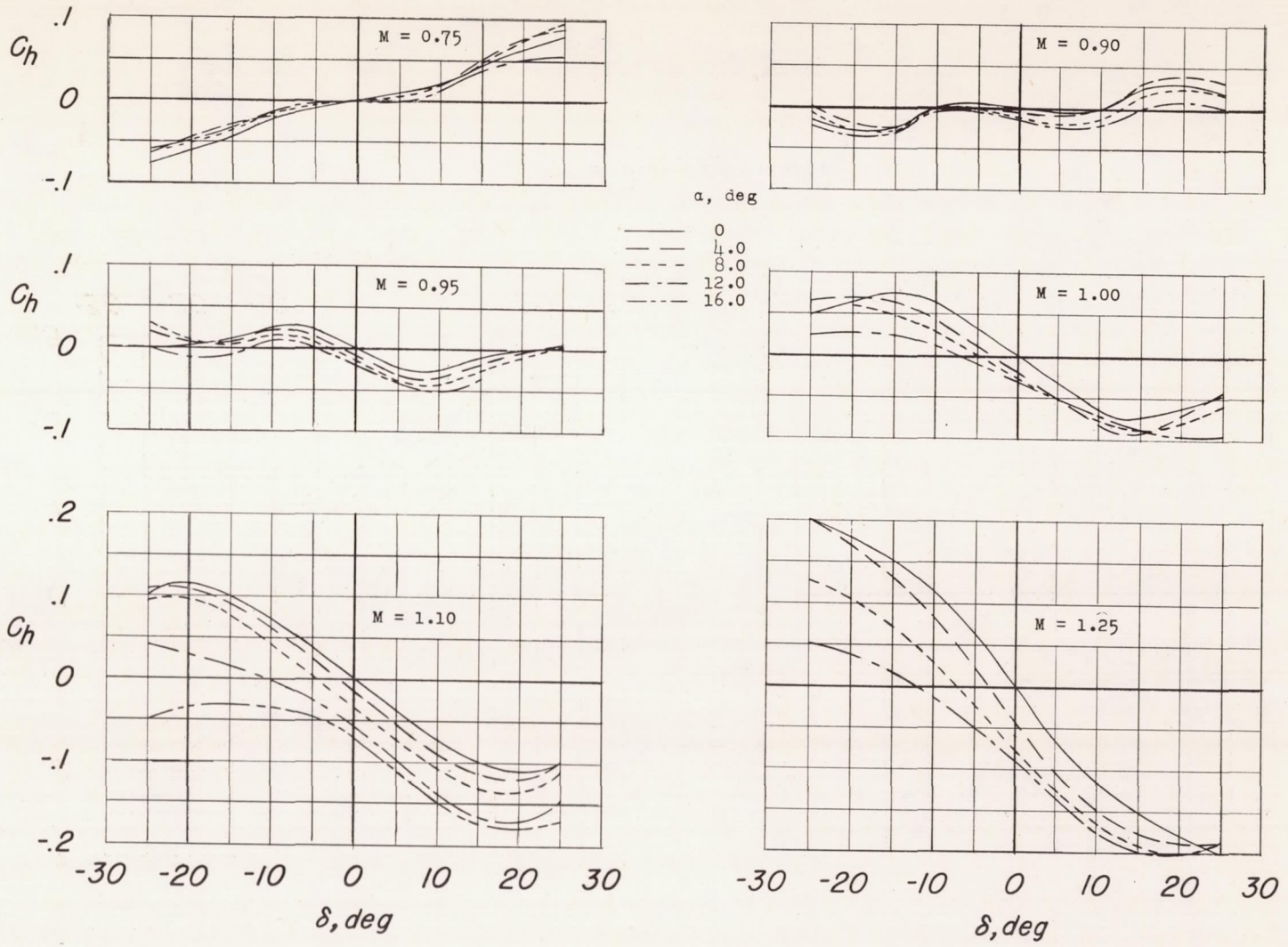

Figure 10.- Variation of control hinge-moment coefficient with deflection at various angles of attack. Balanced control.

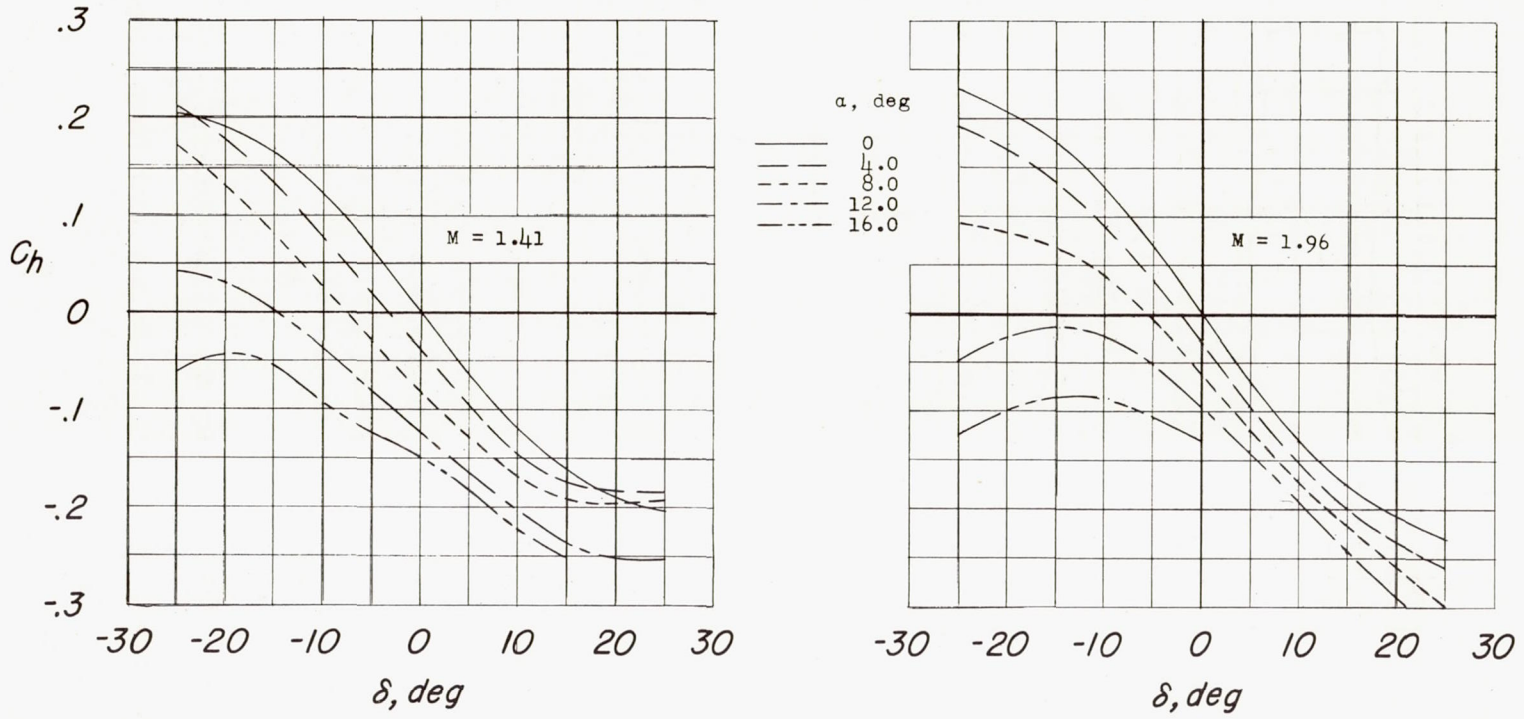

Figure 10.- Concluded.

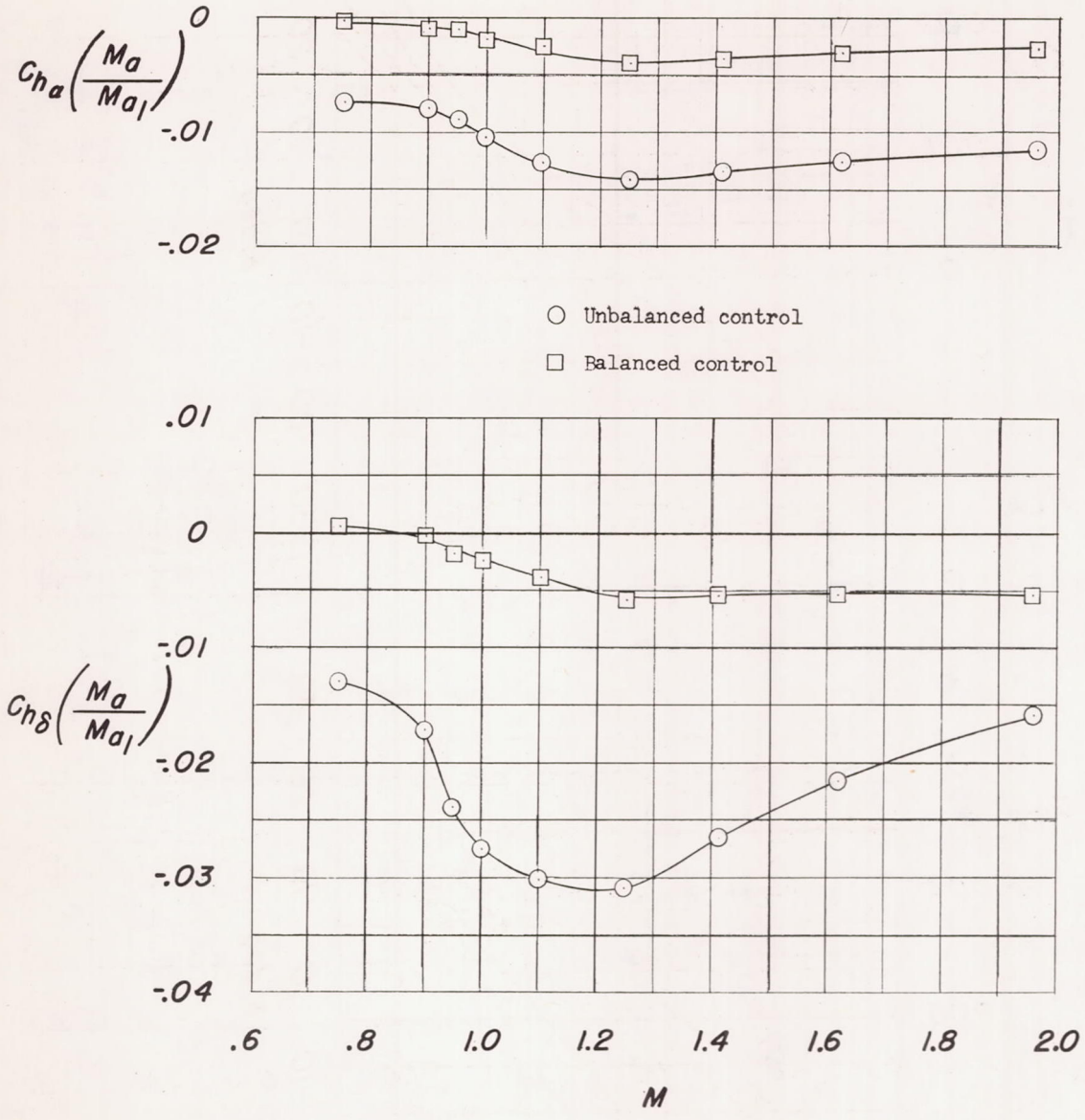

(a) Control hinge moment parameters.

Figure 11.- Variation of control parameters with Mach number for two controls.

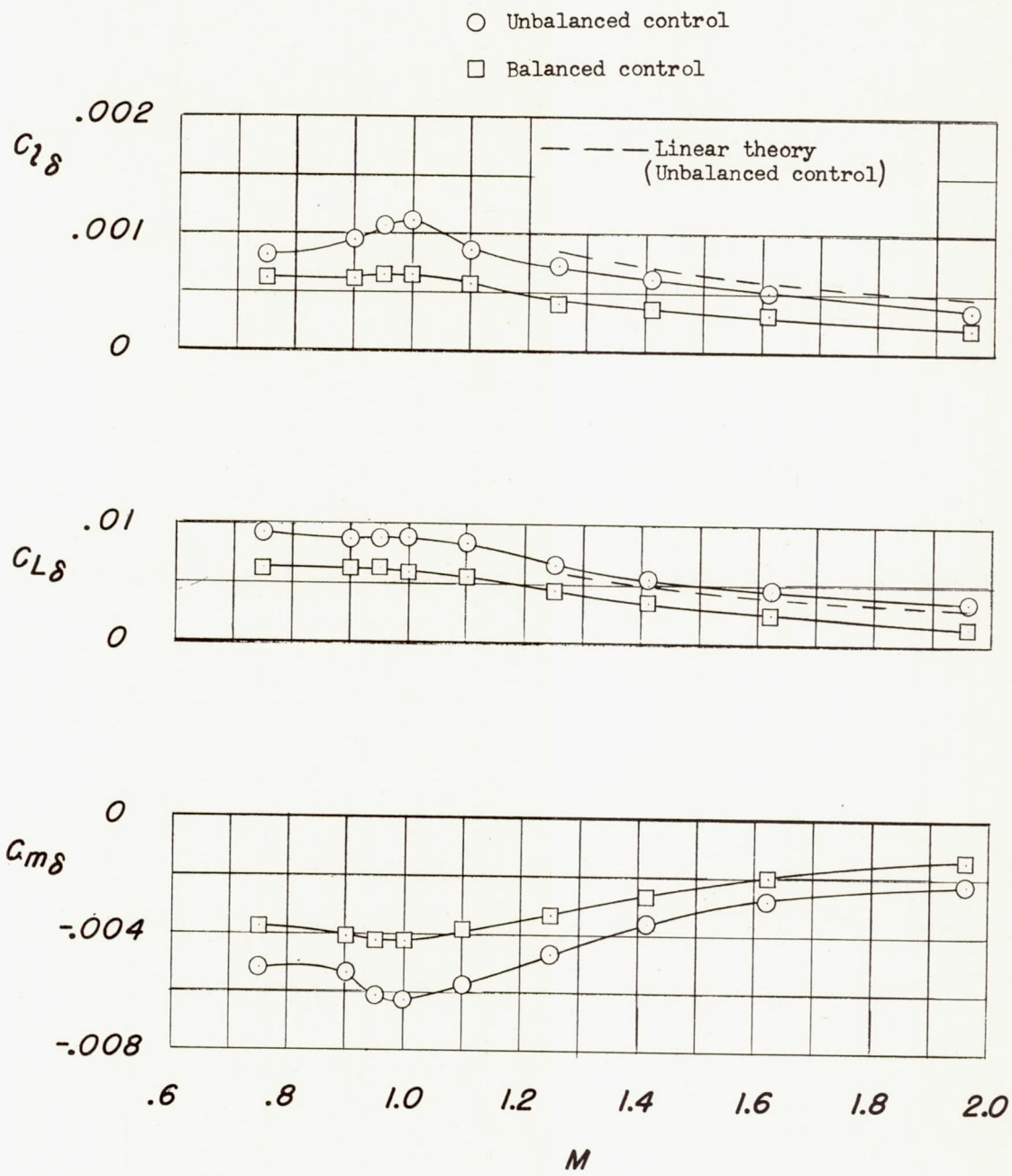

(b) Control effectiveness parameters.

Figure 11.- Concluded.

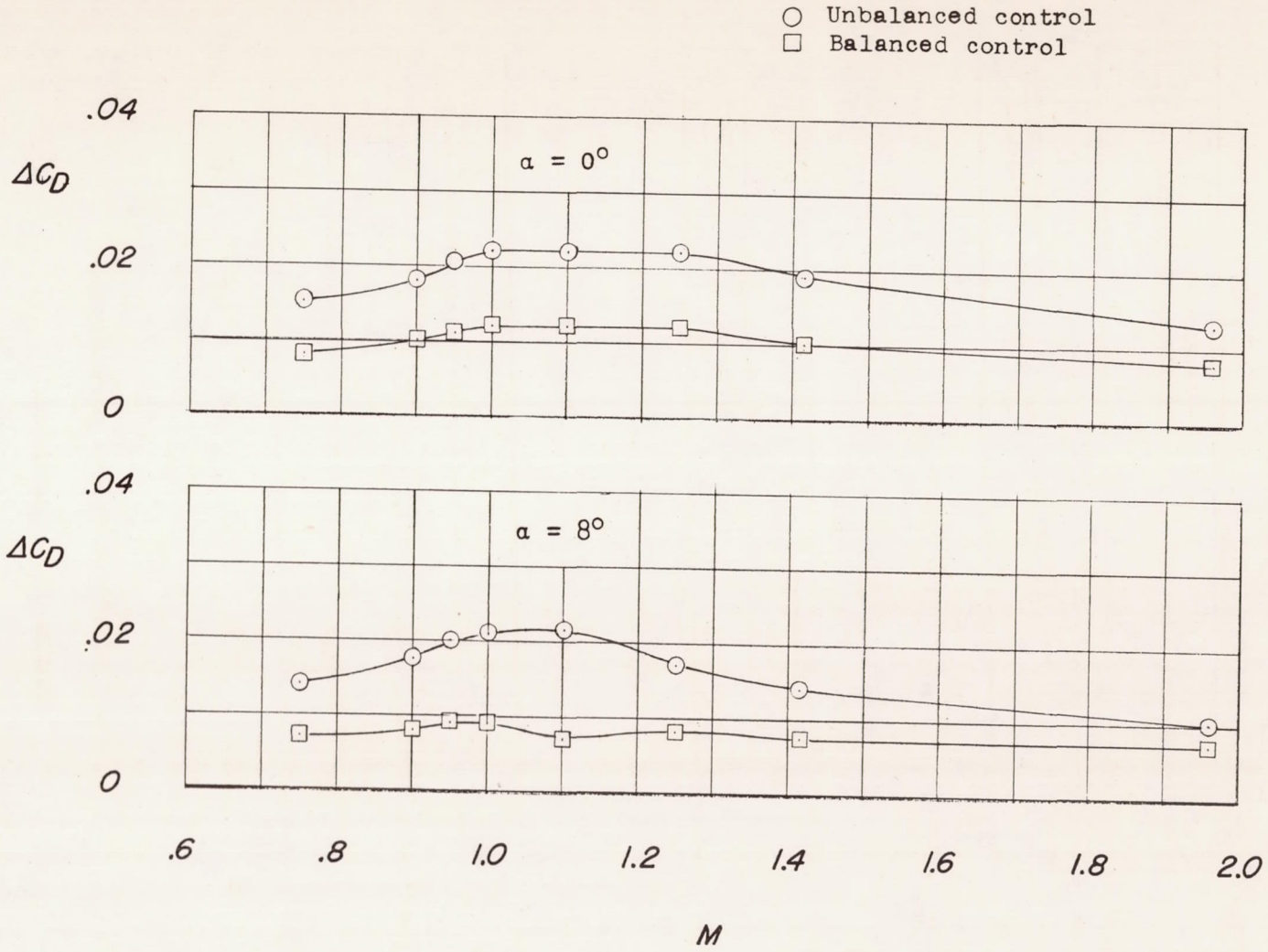

Figure 12.- Variation with Mach number of the incremental drag coefficient due to equal up and down deflection of 10° for two controls.

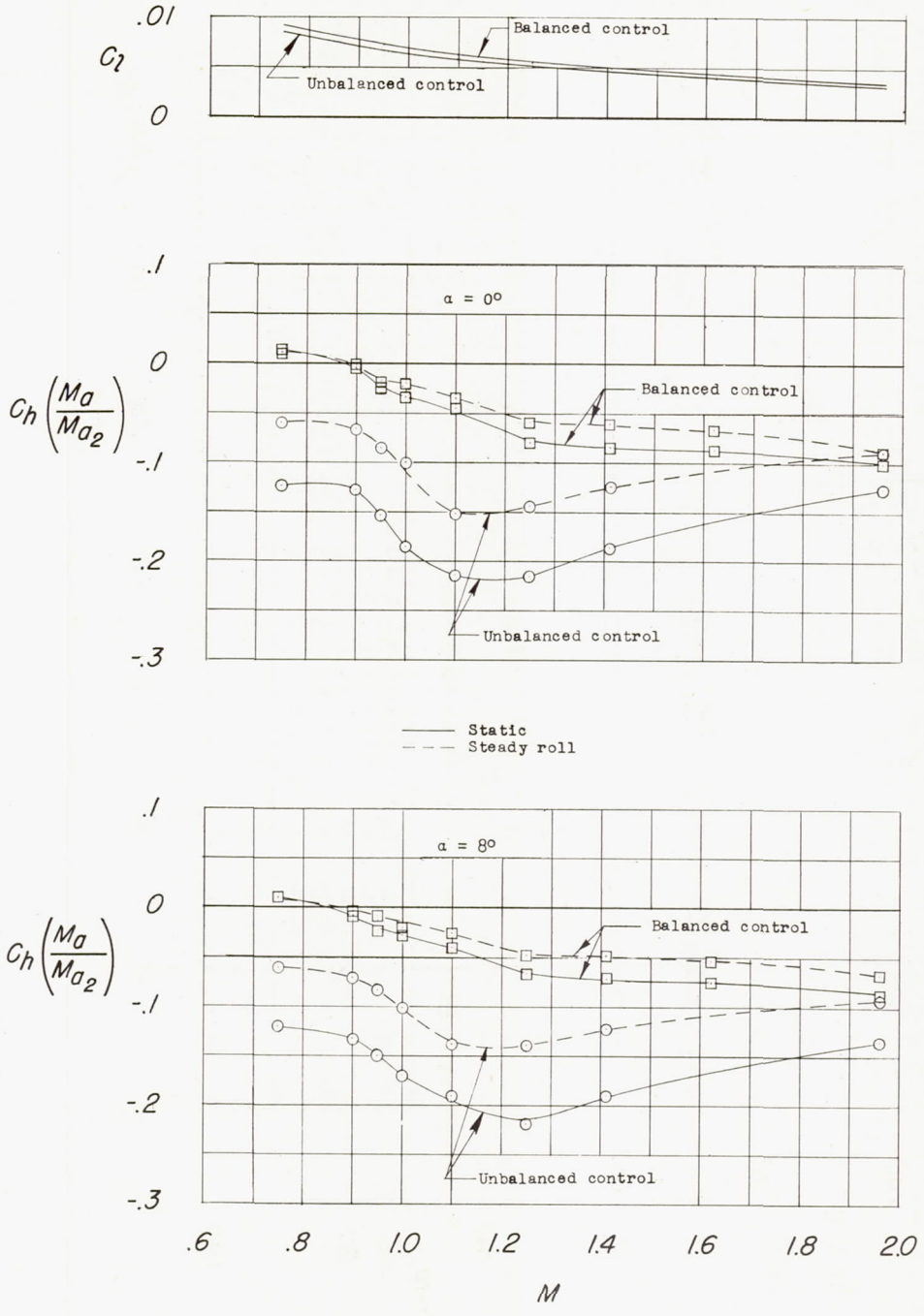

Figure 13.- Comparison of the control hinge-moment coefficient for the balanced and unbalanced control on an 80° swept pointed wing; comparison is made at rolling moments required for 15-radians-per-second roll rates of wings having 204.2 square feet of area and operating at 40,000 feet.

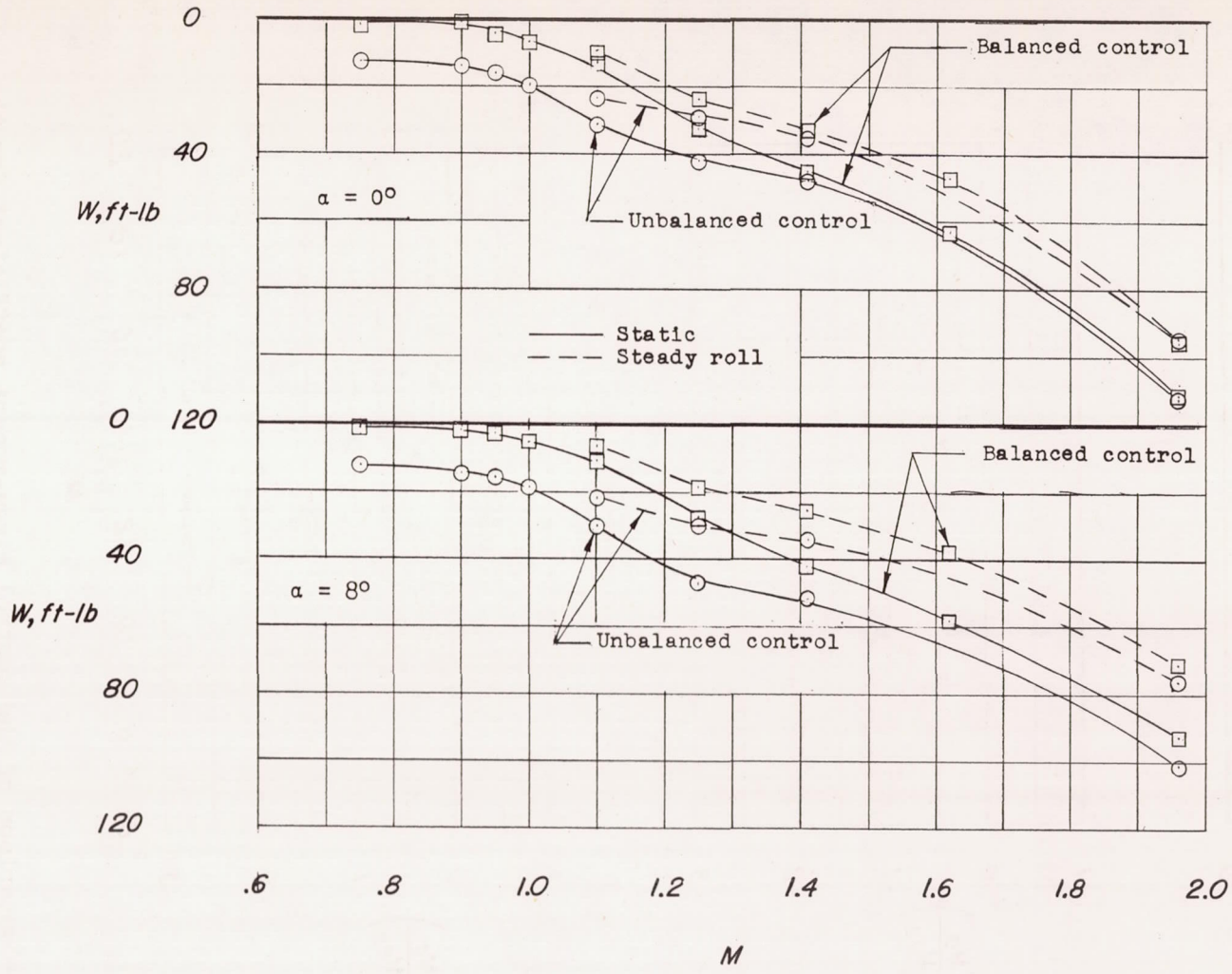

Figure 14.- Comparison of deflection work of two controls producing rolling moments required for 15-radians-per-second roll rates of wings having 204.2 square feet of area and operating at 40,000 feet.